An Automated Finite Element Analysis Framework for the Probabilistic Evaluation of Composite Lamina Properties

A Thesis Presented for the

Master of Science

Degree

The University of Tennessee, Knoxville

Jonathan Phillips Weigand

December 2013

Acknowledgements

I would like to express a deep appreciation for my major professor, Dr. Stephanie TerMaath, who has provided me a remarkable opportunity and foundation to perform exciting and innovative research. She has displayed her unwavering passion and excitement in regard to teaching and research and has been a great personal and academic mentor.

I would also like to thank my committee members, Dr. Edwin Burdette and Dr. Richard Bennett, who have helped to shape my intellectual aspirations and have shown a relentless commitment to excellence.

Without the guidance of these great people, this thesis would not have been possible.

Abstract

This thesis outlines the development of computational modeling tools used to predict the elastic properties of composite lamina from representative volume elements (RVE) using numerical methods. The homogenization approach involves the use of Gauss's Theorem to simply the average volumetric strain integral into a surface integral containing which is defined by surface displacements and their direction. Simulations of RVEs under specific loading conditions (longitudinal tension or shear and transverse tension or shear) are then performed in the software package ABAQUS to obtain the surface displacements. It was found that obtaining quality meshes and applying periodic boundary conditions for each RVE was very user and time-intensive, thus, modeling tools were developed to automate the modeling process. The homogenized composite lamina properties are obtained using C++ code to generate models, batch scripts to run successive simulations in ABAQUS, and C++ code to extract surface displacements from the output data and calculate the final properties. The model generation code contains many user-controllable features such as constituent material properties, fiber volume fraction, mesh density, and type of applied boundary conditions. The modeling tools are then applied in a sensitivity study modeling a unit cell to identify which constituent properties have the largest impact on out-of-plane lamina properties. The framework is then extended to model lamina RVEs consisting of two different fiber materials. The location and percent composition of the two different fiber materials are varied to analyze the effect on out-of-plane lamina properties and identify optimal material combination.

Table of Contents

List of Tables

List of Figures

List of Abbreviations

FRC	fiber reinforced composite
FE	finite element
FEA	finite element analysis
RVE	representative volume element
OFAT	one-factor-at-a-time
GUI	graphical user interface
CSV	comma-separated values

List of Symbols

E_m	elastic modulus of the matrix material
ν_m	Poisson's ratio of the matrix material
E_{1f}	elastic modulus in the x direction of the fiber material
E_{2f}	elastic modulus in the y direction of the fiber material
E_{3f}	elastic modulus in the z direction of the fiber material
ν_{12f}	in-plane Poisson's ratio of the fiber material
ν_{23f}	out-of-plane Poisson's ratio of the fiber material
G_{12f}	in-plane shear modulus of the fiber material
G_{23f}	out-of-plane shear modulus of the fiber material
E_{1L}	elastic modulus in the x direction of the lamina
E_{2L}	elastic modulus in the y direction of the lamina
E_{3L}	elastic modulus in the z direction of the lamina
ν_{12L}	in-plane Poisson's ratio of the lamina material
ν_{23L}	out-of-plane Poisson's ratio of the lamina material
G_{12L}	in-plane shear modulus of the lamina material
G_{23L}	out-of-plane shear modulus of the lamina material
V_F	fiber volume fraction
U	strain energy
$\bar{\sigma}_{ij}$	volumetric average stress tensor
$\bar{\varepsilon}_{ij}$	volumetric average strain tensor
σ_{ij}	stress tensor
ε_{ij}	strain tensor
W	work performed on the system
l	unit cell dimension in the x direction
m	unit cell dimension in the y direction
n	unit cell dimension in the z direction
u_1	boundary displacement in the x direction obtained from ABAQUS
u_2	boundary displacement in the y direction obtained from ABAQUS
u_3	boundary displacement in the z direction obtained from ABAQUS
P_2	normal traction stress applied in the y direction
T_{23}	shear traction stress traction applied in the y-z plane
x	sample mean
s	sample standard deviation
S_1	surface at the fiber-matrix interface of the unit cell
S_2	exterior surface of the unit cell

Chapter 1

Introduction

Motivation

To design optimized and reliable parts manufactured with advanced composite materials customized for particular applications, designers need the capability to efficiently asses the performance of engineered materials and customized composite parts subject to variable loading conditions. Currently, variability in constitutive properties and manufacturing outcomes result in large safety factors for composite parts. A probabilistic based simulation approach that quantifies material and manufacturing uncertainties through multiple scale levels could allow for engineers to more realistically predict composite part performance, develop design guidelines, and limit the costs associated with overdesign and extensive destructive testing programs (Figure 1). A progressive simulation environment would promote recognition of experiments needed to fill in knowledge gaps and provide validation data. Additionally, a fully automated probabilistic-based modeling framework could allow engineers to efficiently analyze many material combinations and configurations using preexisting constituent data.

Research Objective

Fiber reinforced composite (FRC) materials provide customizable structural properties, but predicting and evaluating the response of these materials are difficult due to the nearly unlimited material combinations and configurations used to make composite parts. Consequently, characterizing FRCs through repetitive experimental testing

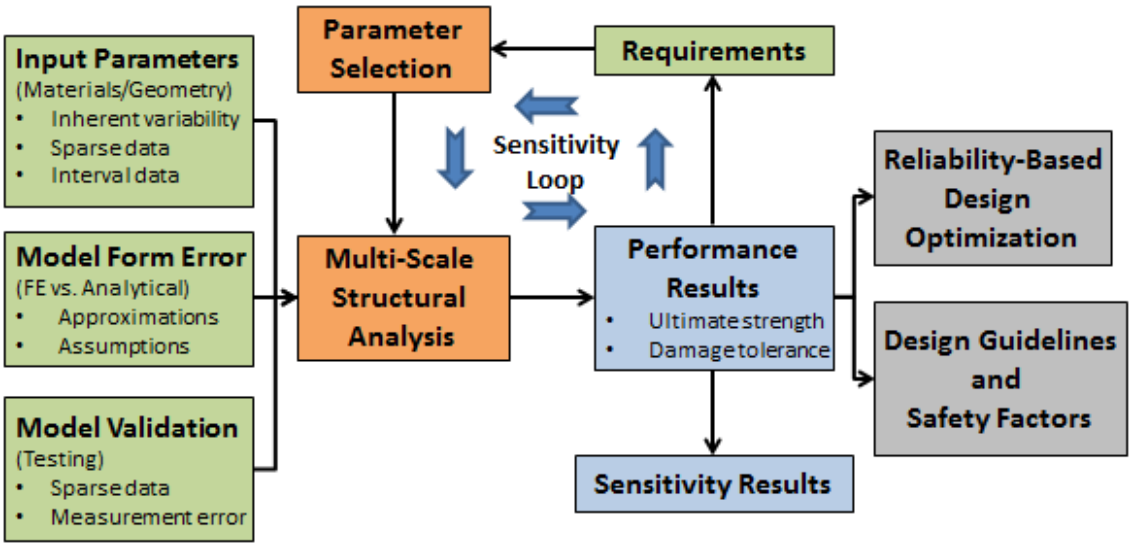

Figure 1. Vision of the Probabilistic Approach to Simulation

programs has proven to be very time-consuming and expensive posing a huge challenge to the industries using composite materials. The most favorable alternative is to characterize effective composite properties using numerical simulation methods that can continuously be refined and built upon to meet the needs of the industry. Therefore, this research is based on a probabilistic multi-scale framework that aims to develop computational tools that allow for efficient design of optimized and reliable composite parts. The framework consists of modeling fiber aligned materials across two scale levels (Figure 2) while incorporating the mechanical behavior and respective uncertainty at each scale level to obtain the effective engineering properties of the final composite material.

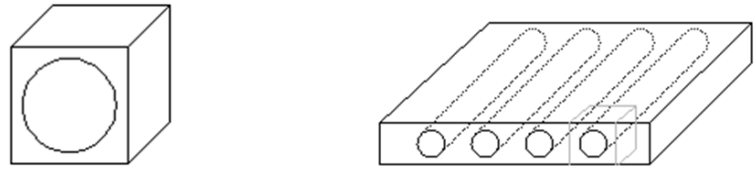

(a) unit cell (b) lamina

Figure 2. Multi-Scale Composite Framework

This thesis demonstrates an automated numerical approach for rapidly assessing unit cell level and lamina level properties within the proposed multi-scale framework. The unit cell consists of a single fiber surrounded by its respective matrix material while the lamina consists of a periodic combination of unit cells. The unit cell approach involves the assumption that the composite cross-section is perfectly periodic, which simplifies the mathematics for analytical formulations and provides for a computationally efficient method for predicting lamina properties [1]. The work presented in this thesis will focus on the development, validation, and application of an automated numerical approach that predicts the effective engineering properties of a composite lamina while capturing the influence of uncertainties in material constitutive properties, lamina configuration, and periodic boundary conditions. The numerical approach consists of user-friendly and readily-expandable computer programs written to rapidly generate a finite element model of a unit cell or representative volume element for a lamina, simulate the response to various loading conditions, and extract the data necessary to calculate homogenized lamina properties.

Thesis Outline

An introduction to fiber reinforced composite materials and composite analysis methods will be discussed in chapter 2 of this thesis. Chapter 3 demonstrates the use of the developed modeling tools to perform an automated sensitivity analysis at the unit cell level to evaluate the influence of constituent properties and geometry on out-of plane lamina properties. The modeling tools consist of code written in C++ programming language to generate input files, automate the simulation process in the finite element code ABAQUS, extract boundary displacements, and calculate homogenized properties. The input file generation code has user-controllable features that allow for different constituent materials, load combinations, and boundary conditions. The results are validated according to analytical and experimental results found in the literature. Chapter 4 entails an extension of the computational tools in which two different fiber materials are introduced in a lamina representative volume element in order to examine the influence on out-of-plane lamina properties and identify the precise combination of fiber types to achieve optimized homogenized properties.

Chapter 2

Composite Material Overview and Literature Review

Composite Material Introduction

Military and industrial applications for fiber reinforced composite (FRC) materials have grown exponentially over the past five decades due to their desirable material properties. These properties include favorable strength to weight ratio, stiffness, and corrosion resistance compared to conventional structural materials such as steel and concrete. FRC materials consist of strong fiber strands embedded in a matrix material that acts to bind fibers together and provide multi-directional strength. Typically, the fibers are placed in the matrix material as continuous fiber strands stacked in multi-directional layers or short randomly distributed fibers (Figure 3).

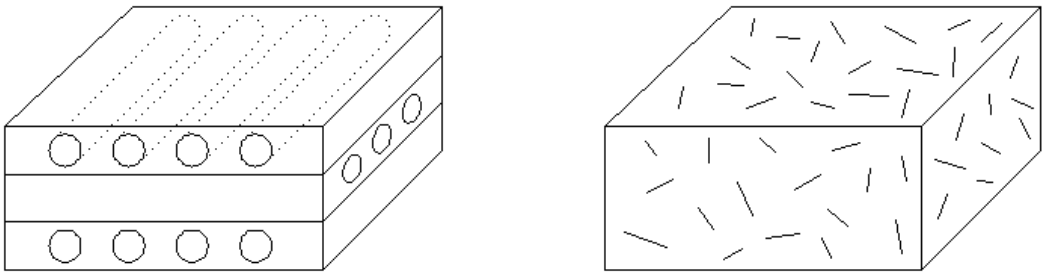

(a) fiber aligned composite (b) randomly oriented short fiber composite

Figure 3. Composite Reinforcement Regimes

With today's manufacturing capabilities, FRCs can be tailored to handle extreme loading and environmental conditions, reduce stress concentrations that arise from bolted

or welded connections, or provide unique performance advantages when combined with other materials such as stainless steel [2]. As a result, FRCs have applications across many disciplines, and they are outlined as follows.

Applications

Aerospace

Structures sent into space such as antennae, optical instrumentation, and mirrors consist of lightweight yet exceptionally stiff graphite composites. These graphite composites are designed to have very low thermal and hygric expansion coefficients which allow them to have a high degree of multi-directional stability in extreme environments [3].

Aircraft

Since the late 1950's, fibrous reinforced materials have been increasingly used in military aircraft because they exhibit high strength-to-weight ratio, low electrical conductivity, high corrosion resistance, and stealth characteristics. Composite materials are increasingly being used for commercial airliners as well. Boeing Aerospace Company is ushering in a new era of commercial aircraft transportation with its new 787 Dreamliner which has an 8,000 mile range and the ability to transport 210-250 passengers in a single flight. The aircraft structure is designed to be roughly 50 percent by weight of carbon-epoxy and graphite-titanium composite, which will provide 20 percent less fuel burn, 30 percent less maintenance cost, and increased reliability compared to similar jets.

Other Applications

Composite material applications also include automotive, marine, energy, infrastructure, armor, biomedical, and recreational sporting. An early application in the automotive industry occurred when GM replaced the steel rear leaf spring in its Corvette with a glass-epoxy spring to reduce the weight [3]. Carbon fiber composite is being used as a strong, lightweight material for newly developed medical and sports equipment. For example, prosthetic limbs are now being manufactured from carbon fiber to make movement more feasible and realistic. Even cycling shoes are being made of a carbon fiber because the material can be heated and shaped specifically for each rider's feet. The applications of FRC composite materials are forever growing and are only limited by the ability to accurately predict structural performance during the design process and efficiently manufacture unique parts.

Analysis Methods Overview

Various methods have been used to predict the effective properties of composite materials, and these methods are broadly categorized as analytical, numerical, or experimental approaches [3]. Theoretical methods provide closed-form expressions allowing for instantaneous homogenized property calculations [1, 4-10]. However, theoretical methods often include gross material or geometric simplifications that result in over-simplified material property prediction particularly in the transverse direction (E_{23L}, ν_{23L}, G_{23L}). Experimental methods are necessary to validate the relation between constituent properties and average lamina properties, but as mentioned before, testing regimes are labor-intensive, time-consuming, and expensive. Numerical approaches have

been shown to provide the most accurate property predictions, but have been considered to be too time-consuming for practical use until recently. Therefore, numerical methods in combination with today's available computing resources provide a favorable alternative to composite material modeling, which is why they were chosen for the focus of this study.

Micromechanical Approach

Having the means to accurately and efficiently predict the effective properties of heterogeneous media is critical to tailoring advanced composite materials. In classical homogenization theory, multi-phase materials such as carbon-epoxy are described in terms of unit cells or representative volume elements (RVE) that imitate the composite microstructure [11]. A unit cell consists of a single fiber and the surrounding matrix material while a lamina RVE consists of multiple fibers surrounded by matrix material. In the literature, the terms unit cell and RVE are sometimes used interchangeably, but Figure 4 displays how each will be defined in this thesis. The unit cell and RVE are sized relative to its constituents to allow for the average properties to remain independent of location within the element. Figure 5 depicts the unit cells most typically used for fibrous composites. Hashin provided an extensive review on periodic RVEs and summarized the concept therein [1]. In theory, boundary conditions can be enforced on a unit cell or RVE such that it is forced to behave as part of larger composite lamina [12-16]. The simplified unit cell or RVE allows for the constituent materials and effective engineering property relation to be efficiently studied through numerical methods.

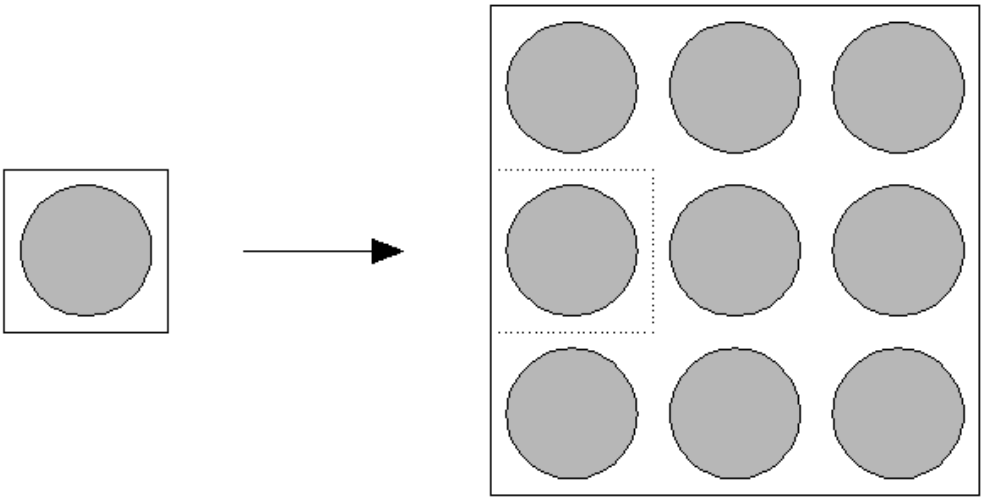

(a) unit cell (b) RVE of lamina

Figure 4. Unit Cell Compared to RVE of Lamina

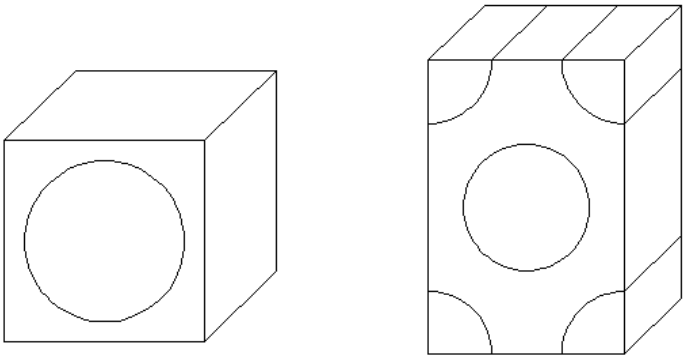

(a) square packing unit cell (b) hexagonal packing unit cell

Figure 5. Typical Unit Cells for FRCs

Boundary Element Method

Overview

The Boundary Element Method (BEM) is a computational method for approximating the solution to partial differential equations posed as equivalent integral equations known as boundary integrals [17]. For a given boundary value problem, boundary conditions are introduced as boundary values in the boundary integrals rather than values throughout the problem domain of the partial differential equation. The boundary integrals can be used to obtain the solution at any point within the problem domain. BEM involves only surface discretization which can render BEM more computationally efficient than volume discretization methods such as the Finite Element Method (Figure 6). For this reason, BEM has been used by researchers to study the material behavior of periodic composite materials. However, BEM was not the method chosen for the focus of this thesis and the reasons why will be discussed at the end of this chapter.

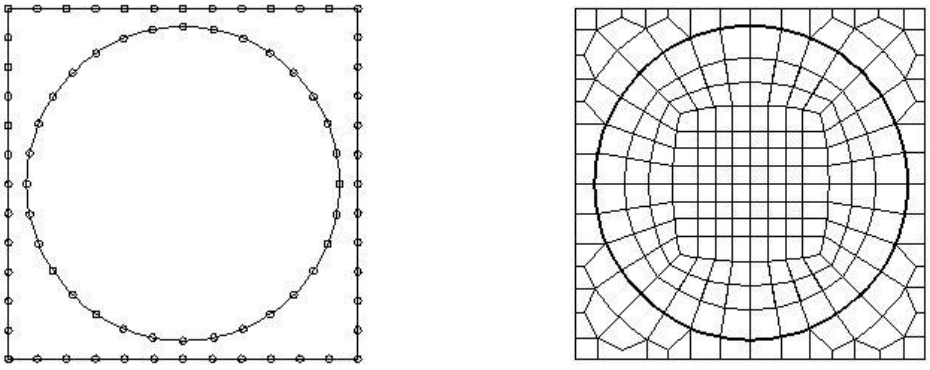

(a) Boundary Element Method (b) Finite Element Method

Figure 6. Comparative Example of Discretization Methods

Implementations

The BEM can provide a straightforward modeling approach when dealing with materials of repetitive microstructure such as FRC composites because of the surface meshing advantages. Kaminski used a BEM based approach to model a RVE of linearly elastic, periodic heterogeneous composite media [18, 19]. The effective elastic constants are computed using strain energy equivalency between the actual configuration and the idealized homogenous medium. The calculated properties were shown to be consistently higher than the properties obtained using FEM-based formulations, and the difference was attributed to the computational procedure used to spatially average the stress tensor components within the RVE.

Okada et al. presented a BEM-based homogenization technique using the method of weighted residuals to derive the integral equations and ultimately the homogenization formulation [20]. The approach involves the assumption that the fiber volume fraction must remain the same across multiple until cells within the local periodic microstructure and that the material constituents must be isotropic.

Chen presented a BEM based technique to study the effects of a third interphase layer located between the fiber and matrix materials [21]. However, the BEM solver was found to run much slower than the commercial FEM software, ANSYS, in which the same analysis was performed.

Finite Element Method

Overview

Like BEM, the Finite Element Method (FEM) is a numerical approach for approximating the solutions to partial differential equations for boundary value problems. Simple shape functions within many discrete subdomains (finite elements) are used to approximate the behavior of a continuous medium. These elemental shape functions allow for field quantity values, such as displacement, to be determined at any location within each element. FEM involves volume discretization rather than surface discretization and provides a natural approach for structural analysis problems. FEM is widely used in the composite modeling community because of its versatility and ability to capture local behavioral effects [22].

Implementations

Blacketter and King utilized a two-dimensional, quarter-symmetric FE model of a RVE to study the effect of matrix and interface properties on the transverse tensile and shear strengths of fiber reinforced materials [23, 24]. Garnich and Karami developed a three dimensional FE model to study the effects of fiber waviness on the structural stiffness and strength properties of fiber reinforced composites [25, 26]. Medeiros modeled multiple RVEs to study the influence of fiber arrangement and shape on homogenized properties [27]. Naik performed a similar analysis on fiber arrangement, but additionally studied bi-directional packing sequences [28].

The literature revealed inconsistencies regarding the correct application of boundary constraints to force a unit cell or RVE to behave as part of a larger composite lamina. Naik, Brockenbrough, and Caruso [29-31] made the assumption that the deformed shape remained plane under transverse shear loading, while Adams and Crane and Sun and Vaidya [32, 33] assumed the deformed shaped did not remain plane (Figure 7). Some researchers have chosen to neglect Poisson's effect due to the notion that boundaries without a primary normal load remain stationary as part of the larger lamina. Many FE modeling approaches have been developed over the past two decades [34-40], yet there is still disagreement in the literature regarding the correct application of boundary displacement constraints.

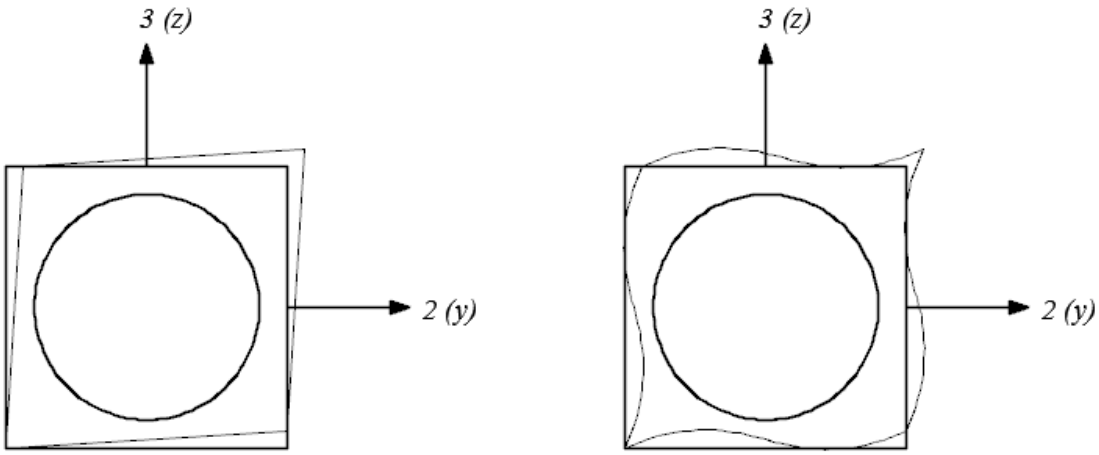

(a) Deformation remains in plane (b) Deformation occurs out of plane

Figure 7. Comparison of Deformed Shape Assumptions

Method Comparison

While BEM may be computationally advantageous in some cases, its applicability is mostly limited to linear problems with simple microstructure [41]. BEM is ill-suited for problems involving nonlinearities or complex micro-geometry such as matrix voids or micro-cracking because each inclusion must discretized separately. The surface discretization scheme creates non-local connectivity in elements rendering fully populated matrices which, as a result, causes computational time to grow exponentially with problem complexity and size. Meanwhile, FEM provides a natural approach for analyzing complex structures across all scales, and because FEM matrices are often banded, computation time grows linearly with problem complexity and size [22]. FEM exhibits superior promise for handling complex micro-geometry such as matrix voids and micro-cracking because discretization of the actual geometry enforces local connectivity of elements. Additionally, FEM has been shown to provide accurate solutions [33, 42] when compared to analytical [1, 10, 43] and experimental [44, 45] results and is available in many commercial packages.

Motivation for an Automated Approach

Many of the models presented in the literature are formulated in two dimensions, involve axis symmetry, and involve conflicting assumptions on the boundary conditions applied to the RVE. The literature has also revealed that computation time, model efficiency, and usability is rarely a focus in the aforementioned numerical approaches, and it has been found that generating quality meshes and applying periodic boundary conditions for RVEs using a FEA software package such as ABAQUS can be a very

meticulous and time-consuming process. Therefore, providing modeling tools that automate the mesh generation process and give the user the ability to control the nature of the applied boundary conditions (e.g. include or neglect Poisson's effect) is a primary task in the development of an automated, probabilistic modeling framework.

Chapter 3

Sensitivity Analysis of Out-of-Plane Composite Properties

Introduction

The futuristic vision for aircraft analysis is a simulation environment where engineers can create and explore unlimited configurations to develop reliable and optimized parts. Currently, the design of customized parts is accomplished through expensive and time-consuming comprehensive test programs. In addition to streamlining material design, an encompassing simulation environment will promote effective design of experiments that will limit material testing, fill in knowledge gaps, and provide quality validation data. With today's computing resources, an automated, probabilistic-based multi-scale numerical modeling framework will allow for composite designers to economically engineer materials, explore material configurations, and optimize part performance.

This chapter outlines the foundation for the framework to achieve the aforementioned vision. Newly developed automated modeling tools are used to perform multi-scale sensitivity analyses and design optimization on proposed material designs through the use of finite element modeling (Figure 8). The computational tools provide the ability to run multiple FEAs, extract displacements from each simulation, and calculate the effective lamina properties with a single initiation of the program. Finite element approaches have been considered user-intensive and computationally demanding. However, the developed computational tool automates the FE modeling

process which allows the user to quickly identify constituent parameters that have the most influence on lamina level properties. To demonstrate the automated modeling tool, a sensitivity analysis is performed to evaluate the influence of constituent properties on effective composite lamina properties. The modeling framework is then extended to investigate composite lamina consisting of variable ratios of two different fiber materials.

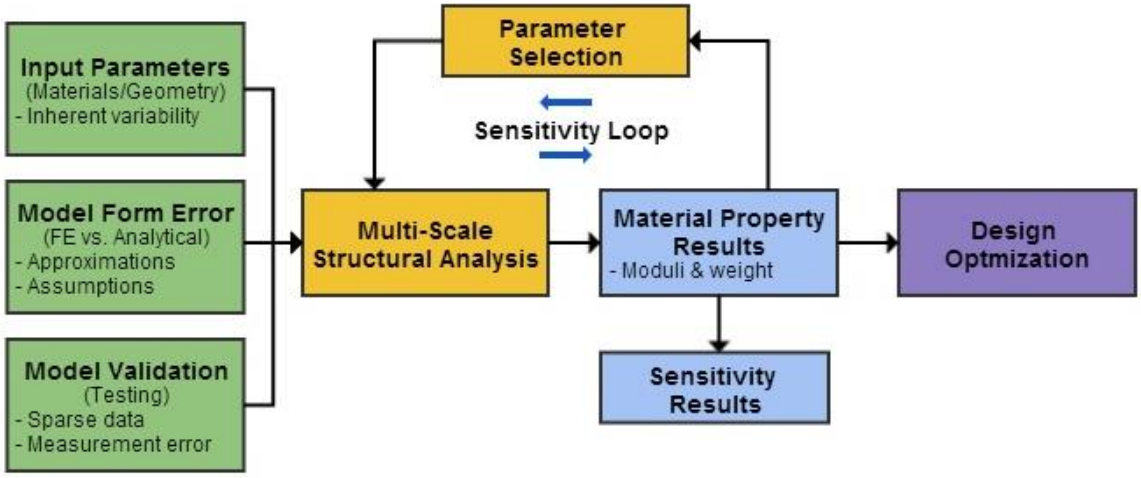

Figure 8. Framework for Sensitivity Analysis and Design Optimization

Model Structure

Automation Framework

Automation of the FE modeling process consists of three main programming tasks: pre-processing to build each customized unit cell or lamina model, scripting to drive successive simulations, and post-processing to extract all necessary data. The pre-processing stage is performed through code written in C++ programming language, which, upon compilation, rapidly generates input files from the following user specified

parameters: degree of mesh density, matrix (E_m and ν_m) and fiber (E_{1f}, E_{2f}, ν_{12f}, ν_{23f}, and G_{12f}) material properties, fiber volume fraction (F_v), load type (longitudinal or transverse tension and shear) and nature of applied boundary conditions (include or neglect Poisson's effect). The major tasks performed by the code consist of generating a quality mesh for each unit cell, defining contact and load surfaces, and defining boundary displacement constraints that enforce periodic behavior in the unit cell or lamina RVE. The meshing algorithm ensures quality element aspect ratios even as the fiber volume fraction exceeds 0.5, which was observed to be very difficult using the graphical user interface (GUI) in ABAQUS. Quality shaped elements located along the fiber-matrix interface will allow for the bond state to be examined in future studies. The automated definition of boundary conditions eliminates the time and possibility of error associated with this essential task. The chosen displacement constraints are discussed in detail in the following section of this paper.

The final portion of the program generates a batch file which contains the scripting necessary to run successive simulations in ABAQUS Standard and create separate comma-separated values (CSV) files containing the surface displacements from each run. The C++ code and batch scripting bypass the need to use the ABAQUS GUI which enables convergence studies to be performed quickly and with minimal user intervention (Figure 9).

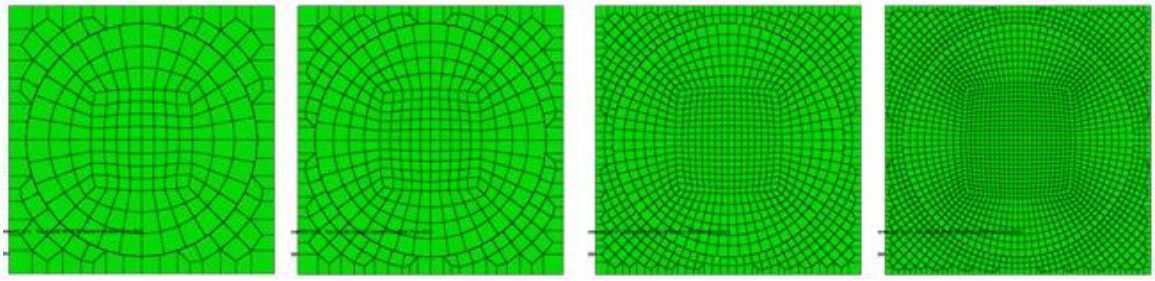

(a) 3,208 elements (b) 6,920 elements (c) 29,368 elements (d) 80,472 elements

Figure 9. Example Meshes Generated for Convergence Study

Table 1 contains a summary of a mesh convergence study. The displacement terms (u_1, u_2, and u_3) are the boundary displacements in the principal directions obtained from longitudinal tension, transverse tension, and transverse shear load conditions. The purpose for these load conditions and displacements will be discussed later in this chapter. It was determined that mesh c provided both suitable displacement convergence and computational efficiency.

Table 1. Summary of Convergence Study

Mesh Density Details			Longitudinal Tension		Transverse Tension		Transverse Shear
Mesh	Elements	Avg. Run (sec)	u_1 (mm)	$u_2 = u_3$ (mm)	u_2 (mm)	u_3 (mm)	$u_2 = u_3$ (mm)
a	3,208	3	0.0483	-0.0122	0.7151	-0.2501	1.1166
b	6,920	6	0.0482	-0.0122	0.7150	-0.2503	1.1142
c	29,368	20	0.0481	-0.0121	0.7145	-0.2502	1.1111
d	80,472	120	0.0481	-0.0121	0.7143	-0.2502	1.1099

The final portion of the modeling tool is a C++ program that retrieves the boundary displacements and runtime from each simulation, calculates the effective (homogenized) elastic lamina properties, and outputs the lamina properties, constituent properties, and runtime into a single CSV file. This comma-separated value file displays the all results in column fashion in spreadsheet management software (Microsoft Excel) such that the correlation between the constituent properties and lamina properties can be readily examined. Ultimately, the modeling tools permit users to obtain all six independent elastic lamina properties (E_{1L}, E_{2L}, ν_{12L}, ν_{23L}, G_{12L}, and G_{23L}) in a single initiation of the program.

Finite Element Model

Homogenization Approach

The distribution of fibers within an actual composite lamina is random through the cross-section. However, most micromechanical models simplify the micro-geometry by assuming a periodic fiber arrangement allowing for a single unit cell or RVE to characterize the lamina. The unit cell for this analysis consists of a single fiber surrounded by its respective matrix material indicative of a square packing sequence (Figure 10).

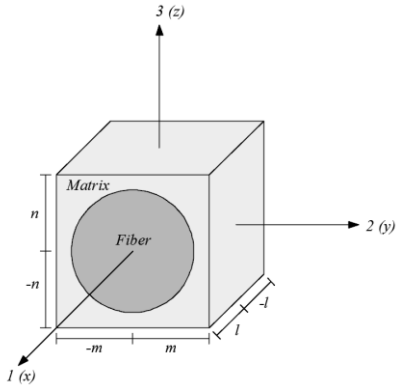

Figure 10. Depiction of the Unit Cell and Coordinate System

Examining the behavior of the unit cell subject to longitudinal (in-plane) and transverse (out-of-plane) loading schemes can give insight into the lamina level behavior. Because the elastic properties of the fiber and matrix material are usually quite different, the stress and strain fields resulting from uniform loading are not uniform as in a homogenous medium. Therefore, special measures must be taken in order to confirm that simple stress and strain relations may be used to calculate the average elastic properties of the two combined materials.

Sun and Vaidya [33] formulated a homogenization approach by proving that the strain energy stored homogenous unit cell (eq. 1-3) is equal to that in a heterogeneous unit cell provided that perfect bonding occurs at the fiber-matrix interface (eq.1).

$$U = \frac{1}{2}\int_v \sigma_{ij} \cdot \varepsilon_{ij} \cdot dV \tag{1}$$

$$\bar{\sigma}_{ij} = \frac{1}{V}\int_V \sigma_{ij}(x,y,z)dV \tag{2}$$

$$\bar{\varepsilon}_{ij} = \frac{1}{V}\int_V \varepsilon_{ij}(x,y,z)dV \tag{3}$$

Because all unit cells are assumed to be identical across the composite section, the stress and strain gradients resulting from uniform loading conditions are periodic. The average volumetric strain within the unit cell is related to the boundary displacements through Gauss's Theorem, which relates the flow of a vector field through a surface to the behavior of the internal vector field. Gauss's Theorem allows for the average volumetric strain in the heterogeneous unit cell to be converted to surface integrals that occur at the outer fiber surface (S_1), inner matrix surface (S_1), and outer matrix surface (S_2). The surface integrals are characterized by the displacement at the surface and the unit normal (direction) of the displacement. The two surface integrals along the fiber matrix interface are equal and opposite, which results in a final surface integral that contains only boundary displacements and the associated unit normals (eq.4).

$$\begin{aligned}\bar{\varepsilon}_{ij} &= \frac{1}{V}\left(\frac{1}{2}\int_{S_2}(u_i n_j + u_j n_i)dS + \frac{1}{2}\int_{S_1}(u_i n_j + u_j n_i)dS - \frac{1}{2}\int_{S_1}(u_i n_j + u_j n_i)dS\right) \\ &= \frac{1}{2V}\int_{S_2}\left(u_i n_j + u_j n_i\right)dS\end{aligned} \tag{4}$$

Because surface displacement constraints are enforced on the unit cell such that all surface displacements are known, only these boundary displacements are needed to calculate the average volumetric strain ($\bar{\varepsilon}_{ij}$). This approach is favorable because obtaining the surface displacements is much less rigorous than attaining the strain in every element. This average volumetric strain can then be used to determine the homogenized (averaged) properties.

Longitudinal and Transverse Tension Loading

A longitudinal tension load is modeled by a uniform load (P_1) acting on the front and back faces ($x = \pm l$) of the unit cell, while a transverse tension load is modeled by a uniform load acting on the right and left faces ($y = \pm m$) of the unit cell (Figure 11). The boundary displacement constraints are specified in the FE model as such,

$$u_1(l,y,z) = -u_1(-l,y,z)$$
$$u_2(x,m,z) = -u_2(x,-m,z) \quad (5)$$
$$u_3(x,y,n) = -u_3(x,y,-n)$$

where u_1, u_2, and u_3 are the surface displacements in the x, y, and z directions computed with FEA. These boundary conditions allow contraction due to Poisson's effect.

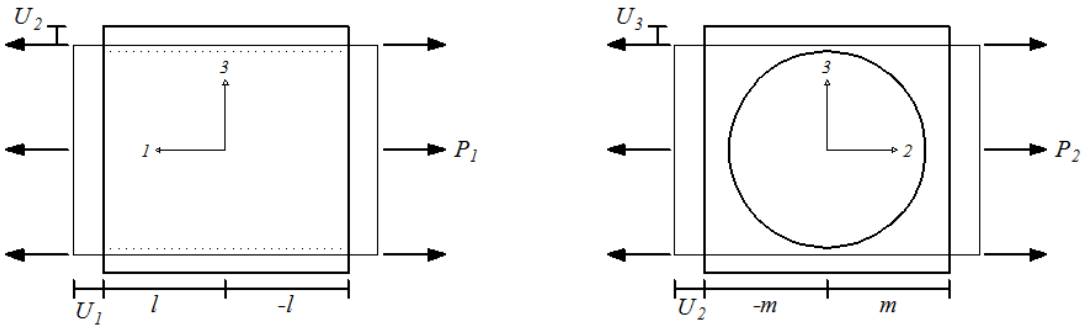

(a) Longitudinal Tension (b) Transverse Tension

Figure 11. Normal Loads and Displacements for FEA Unit Cell Model

The surfaces are assumed to remain plane during normal loading in order to force compatible behavior of the unit cell (Figure 10).

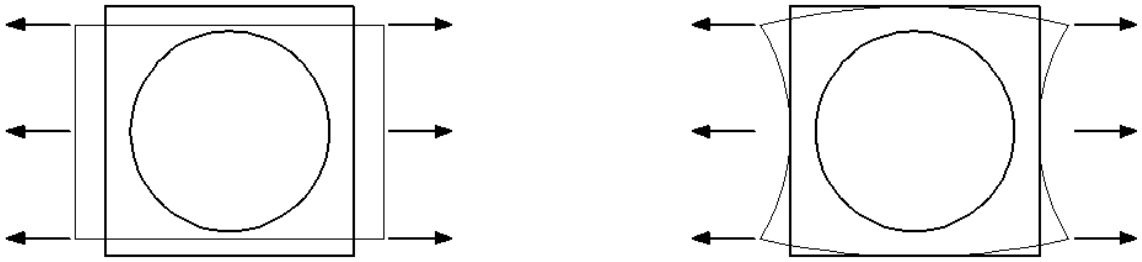

(a) Compatible deformation (b) Incompatible deformation

Figure 12. Compatible Deformation of the Unit Cell

Continuing to follow Sun and Vaidya [33] for the longitudinal tension load case, the average longitudinal is calculated using the definition of strain.

$$\bar{\varepsilon}_{11} = \frac{u_1}{l} \tag{6}$$

The internal strain energy stored in the unit cell is equated to:

$$U = \frac{1}{2}\bar{\sigma}_{11} \cdot \bar{\varepsilon}_{11} \cdot V \tag{7}$$

The external work performed on the unit cell by the uniform load is formulated by:

$$W = \frac{1}{2}P_1 \cdot 2m \cdot 2n \cdot 2u_1 \tag{8}$$

Equating the two according to the work-energy principal results in:

$$\frac{1}{2}\bar{\sigma}_{11} \cdot \bar{\varepsilon}_{11} \cdot V = \frac{1}{2}P_1 \cdot 2m \cdot 2n \cdot 2u_1 \tag{9}$$

By substituting eq. (6) into eq. (9), the average stress in the longitudinal direction is proven to equal the applied uniform tensile load:

$$\bar{\sigma}_{11} = P_1 \tag{10}$$

Thus, the effective longitudinal modulus and Poisson's ratio are calculated as

$$E_{1L} = \frac{P_1 \cdot l}{u_1} \qquad \text{and} \qquad \nu_{12L} = -\frac{u_2}{u_1} \tag{11}$$

because the unit cell side lengths are identical. In a similar fashion, the transverse modulus and Poisson's ratio are determined by:

$$E_{2L} = \frac{P_2 \cdot m}{u_2} \qquad \text{and} \qquad \nu_{23L} = -\frac{u_3}{u_2} \tag{12}$$

Transverse Shear Loading

A transverse shear load is modeled by counter-clockwise surface tractions on the right and left surfaces ($y = \pm m$) and clockwise surface tractions on the top and bottom surfaces ($z = \pm n$) of the unit cell (Figure 10). Sun and Vaidya analyzed a 3 by 3 cell model subject to transverse shear in order to determine the correct boundary displacement constraints to place on the RVE [33]. The middle cell is typically used as the representative cell because it is adequately distanced from the free edges. The analysis results revealed that the surfaces of the middle cell do not remain plane as assumed in previous modeling approaches [29-31] and that only periodicity and symmetry conditions need to be satisfied.

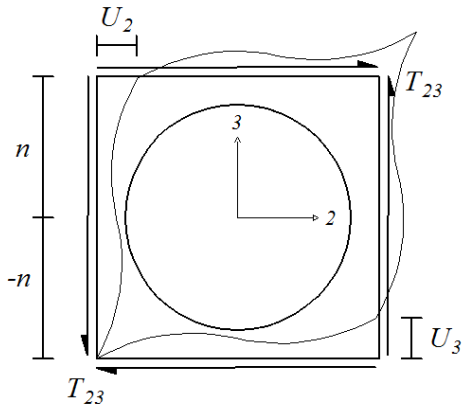

Figure 13. Transverse Shear Load and Displacements for FEA Unit Cell Model

Therefore, the boundary displacement constraints applied to the unit cell are determined as such:

$$u_1(l,y,z) = -u_1(-1,y,z)$$

$$u_3(x,m,z) = -u_3(x,-m,z) \qquad u_2(x,m,z) = u_2(x,-m,z) \tag{13}$$

$$u_2(x,y,n) = -u_2(x,y,-n) \qquad u_3(x,y,n) = u_3(x,y,-n)$$

Sun and Vaidya also determined that lateral straining does not occur at the boundaries of the middle cell [33]. Therefore, the RVE surface displacements in the directions of the applied traction forces are defined to remain constant.

$$u_3(x,\pm m,z) = constant \qquad u_2(x,y,\pm n) = constant \tag{14}$$

With the applied boundary displacement constraints, the average transverse shear strain is calculated as:

$$\bar{\gamma}_{23} = \frac{1}{V}\int_V \gamma_{23} \cdot dV = 2 \cdot \frac{u_2}{n} \tag{15}$$

Equating the internal strain energy with the work done on the unit cell:

$$\frac{1}{2}\bar{\sigma}_{23}\cdot\bar{\gamma}_{23}\cdot V = 4\cdot\frac{1}{2}T_{23}\cdot 2m\cdot 2n \tag{16}$$

By substituting eq. (15) into eq. (16), it is proven that the average transverse shear stress is equal to the applied shearing stress:

$$\bar{\sigma}_{23} = T_{23} \tag{17}$$

Therefore, the transverse shear modulus is calculated as follows:

$$G_{23} = \frac{T_{23}\cdot n}{U_2} \tag{18}$$

Validation of Predicted Properties

A carbon-epoxy composite lamina is chosen to validate the unit cell model because of the availability of test data. The independent AS4 carbon fiber and 3501-6 epoxy material properties used in the analysis are displayed in Table 1.

Table 2. Mechanical Properties of Fiber and Matrix Materials

Ref. [23]	E_1 (GPa)	E_2 (GPa)	ν_{12}	ν_{23}	G_{12} (GPa)
AS4 Carbon	235	14	0.20	0.25	28
3501-6 Epoxy	4.8	4.8	0.34	0.34	1.8

The elastic lamina properties obtained from the finite element model are compared to analytical and experimental results found in the literature. Hashin [1] and Whitney and Riley [43] attained results using an analytical approach based on energy principals. Sun [42] and Chamis [10] formulated an approach based on micromechanics which utilized displacement constraints and force equilibrium conditions. Meanwhile, Daniel and Lee [45] and Sun and Zhou [44] performed an experimental investigation to estimate the

effective elastic composite properties. Sun and Vaidya [33] validated the boundary displacement constraints applied to the unit cell model by building a RVE model consisting of multiple fibers to examine the deformed shape of a centrally located cell.

Following the approach formulated by Sun and Vaidya, the modeling tools coupled with ABAQUS generated results that showed substantial agreement with analytical and experimental results found in the literature (Table 3). The out-of-plane lamina properties extracted from the FEA are further compared to results obtained using the self-consistent Field method (eq. 19). The property comparison between the FEA and analytical equations are presented in Table 4. While the analytical equations yield in-plane properties that agree quite well, the predicted out-of-plane properties differ substantially from both the FEA results and previous validation results. The deviation is introduced by the out-of-plane lamina bulk modulus (K_2) term which propagates through the remaining out-of-plane properties. This comparison is performed to illustrate that the two analysis methods are generating considerably different results.

Table 3. Mechanical Properties of Carbon/Epoxy Composite Lamina (Fv=0.6)

Elastic Property (GPa)	FEA	Ref. [33]	Ref. [1]	Ref. [43]	Ref. [42]	Ref. [10]	*Ref. [45]	*Ref. [44]
E_{1L}	142.7	142.6	142.9	142.9	142.6	142.9	142.0	139.0
E_{2L}	9.61	9.60	9.40	9.78	9.20	9.79	10.30	9.85
G_{23L}	3.09	3.10	3.42	-	-	3.01	3.80	-
v_{12L}	0.25	0.25	0.25	0.25	0.26	0.26	-	0.30
v_{23L}	0.35	0.35	0.39	-	-	0.42	-	-

* experimental data

$$G_{23} = \frac{G_m[K_m(G_m + G_{23f}) + 2G_{23f}G_m + K_m(G_{23f} - G_m)V_f]}{K_m(G_m + G_{23f}) + 2G_{23f}G_m - (K_m + 2G_m)(G_{23f} - G_m)V_f}$$

$$E_1 = V_f E_{1f} + V_m E_m + \frac{4(v_m - v_{12f})^2 K_f K_m G_m V_m V_f}{K_f K_m + G_m(V_f K_f + V_m K_m)}$$

$$v_{12} = V_f v_{12f} + V_m v_m + \frac{(v_m - v_{12f})(K_m - K_f)G_m V_m V_f}{K_f K_m + G_m(V_f K_f + V_m K_m)}$$

$$v_{23} = 1 - \frac{E_2}{2K_2} - 2v_{12}^2 \frac{E_2}{E_1} \qquad E_2 = \frac{1}{\frac{1}{4K_2} + \frac{1}{4G_{23}} + \frac{v_{12}^2}{E_1}}$$

$$G_{12} = G_m \frac{(1 + V_f)G_{12f} + V_m G_m}{V_m G_{12f} + (1 + V_f)G_m} \qquad K_2 = \frac{(K_{2f} + G_m)K_m + (K_{2f} - K_m)G_m V_f}{(K_{2f} + G_m) - (K_{2f} - K_m)V_f}$$

$$K_m = \frac{E_m}{2(1 + v_m)(1 - 2v_m)} \qquad K_f = \frac{E_{1f}E_{2f}}{2(1 - v_{23f})E_{1f} - 4v_{12f}^2 E_{2f}}$$

(19)

Table 4. Comparison of Lamina Properties Obtained from FEA and Self-Consistent Field Method

Method	E_{1L}	E_{2L}	v_{12L}	v_{23L}	G_{23L}
FEA	142.7	9.61	0.25	0.35	3.09
Analytical	142.9	9.10	0.25	0.38	3.29

Investigation of Poisson's Effect

Some researchers have assumed that cell boundaries on which no normal load acts are forced to remain stationary as part of the larger lamina and have chosen to neglect Poisson's effects (Figure 14).

(a) Including Poisson's effect (b) Neglecting Poisson's effect

Figure 14. Comparison of Deformed Shape with and without Poisson's Effect

Therefore, the code is formulated with an option to include or neglect Poisson's effect allowing for easy comparison with analytical or experimental results. The omission of Poisson's effect yielded a substantial increase in the transverse tensile modulus of the lamina (Table 5) and cause for a significant reduction in the maximum effective stress developed in the fiber (Figure 15). This behavior occurs because there is more volume to resist the applied normal stress. Including Poisson's effect yield lamina properties much closer to those found in the literature (Table 3); therefore, Poisson's effect is included in all further analyses.

Table 5. Comparison of Lamina Properties Relative to Boundary Conditions (GPa)

Boundary Conditions	E_{1L} (GPa	E_{2L}	ν_{12L}	ν_{23L}	G_{23L}
Include Poisson's Effect	142.7	9.61	0.25	0.35	3.089
Neglect Poisson's Effect	144.6	11.05	0	0	3.089
Percent Increase	1.3%	15.0%	-	-	0.0%

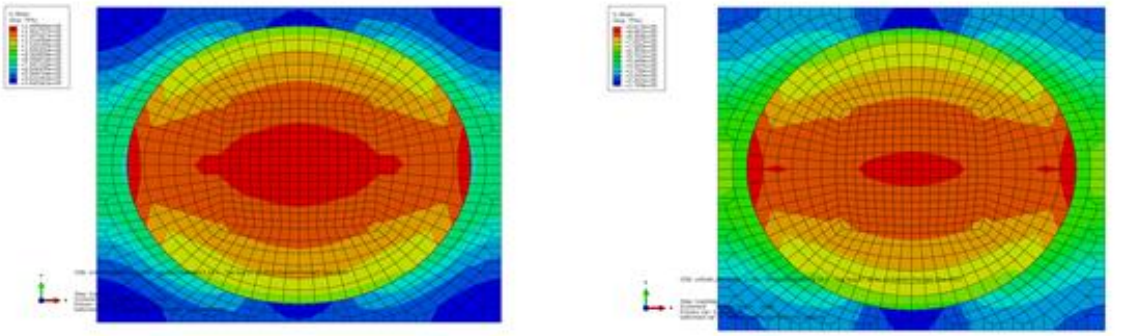

(a) Included Poisson's effect
max stress = 1,496 GPa

(b) Neglected Poisson's effect
max stress = 962 GPa

Figre 15. Comparison of von Mises Stress with Varying Boundary Conditions

Single Variant Sensitivity Analysis

Core Methodology

Typically in aircraft design and analysis, the effects of out-of-plane shear modulus, G_{23}, and Poisson's ratio, ν_{23}, on structural behavior are omitted, or these properties are roughly estimated. Understanding the sensitivity of structural performance results relative to these two properties will lead to effective test plans and improved structural analysis. A high sensitivity indicates that it is worth the time and resources for thorough material testing to obtain out-of-plane properties for each specific composite. If

it is determined that structural behavior is not sensitive to these out-of-plane properties, then designers and analysts can continue using current assumptions and methods with confidence. Behaviors that may be sensitive to out-of-plane properties include bearing, interlaminar stresses due to temperature loading, crack propagation, buckling, and stress distributions around holes. These complex and less understood material interactions are why out-of-plane composite properties (E_{2L}, v_{23L}, and G_{23L}) are chosen for the focus of this sensitivity study.

A single variant sensitivity analysis is performed according to the one-factor-at-a-time (OFAT) methodology to examine the effect of constituent properties on out-of-plane lamina properties. One constituent parameter is varied while all others are held at a baseline value in order to monitor the influence of the single variant. The parameter is returned to a baseline value before the next parameter is subject to variation. An extensive overview of sensitivity analysis methods including OFAT is presented by Hamby [46]. Performing a sensitivity analysis through FEA can be considered time-consuming, but the automation capabilities of the developed computational tools eliminate all user-intensive tasks associated with FEA of fibrous composites. A carbon-epoxy composite material is once again used to demonstrate the usefulness and efficiency of the automated modeling framework.

Determination of Input Parameter Range

An extensive literature search for the material properties of AS4 carbon and 3501-6 epoxy resin revealed that available experimental test data is limited and inconsistent. The sparseness and questionable validity of the available constituent data makes carbon-

epoxy an exemplary material for investigation. The mean and standard deviation are used to establish a representative range for the two matrix properties (E_m, ν_m), five independent fiber properties (E_{1f}, E_{2f}, ν_{12f}, ν_{23f}, G_{12f},), and the fiber volume fraction (V_F). The lower and upper bounds for each parameter are calculated as three standard deviations on either side of the calculated mean. The data collection and calculated bounds are presented in Tables 6 and 7.

The collected data revealed no variability in both the in and out-of-plane Poisson's ratio of the carbon fiber; therefore, a lower and upper bound are approximated. Meanwhile, the data collected for the in-plane shear modulus of the fiber (G_{12f}) followed a bimodal distribution. Therefore, an equivalent mean and standard deviation are calculated to span three deviations above and below the two observed means. These equivalent values are subsequently used in the input file generation code to establish a range for G_{12f}. The fiber volume fraction for the carbon-epoxy is selected to range from 0.5 to 0.7 as this is the range most often mentioned in the literature [3]. The mean values for all input properties are used to establish a baseline set of elastic lamina properties. Next, six FE simulations are performed over each input property range according to the OTAF methodology to evaluate the sensitivity of each out-of-plane lamina property.

Results and Discussion

The sensitivity results of the three out-of-plane lamina properties (E_{2L}, ν_{23L}, G_{23L}) relative to the eight independent constituent properties (E_m, ν_m, E_{1f}, E_{2f}, ν_{12f}, ν_{23f}, G_{12f}, F_v) are displayed on the following pages in Figures 16-18. The relative influence of each input property is readily observed through the slope of each graph.

Table 6. 3501-6 Epoxy Resin Properties from Literature Search

Reference	E_m (GPa)	ν_m
[47]	4.2	0.34
[26]	4.3	0.35
[48]	4.3	0.34
[24]	4.4	0.34
[49]	4.2	0.34
[50]	4.4	0.34
[51]	4.8	0.34
[52]	4.2	-
[3]	4.3	0.35
Mean	4.349	0.343
Calculated *s*	0.184	0.005
Lower Bound	3.796	0.329
Upper Bound	4.902	0.356

Table 7. AS4 Carbon Fiber Properties from Literature Search

Reference	E_{1f} (GPa)	E_{2f} (GPa)	ν_{12f}	ν_{23f}	*G_{12f} (GPa)
[53]	224.0	14.0	0.20	0.25	14.0
[10]	213.7	13.8	0.20	0.25	13.8
[47]	225.0	15.0	0.20	-	15.0
[54]	234.0	14.0	-	-	-
[55]	228.0	-	-	-	-
[56]	231.0	-	-	-	-
[24]	221.0	13.8	0.20	0.25	13.8
[3]	235.0	15.0	0.20	-	27.0
[57]	231.0	-	-	-	-
[23]	235.0	14.0	0.20	0.25	28.0
[58]	235.0	-	-	-	-
[48]	235.0	14.0	0.20	-	28.0
Mean	229.0	14.20	0.200	0.250	14.15 (27.67)
Calculated *s*	6.86	0.501	0.000	0.000	0.574 (0.577)
Effective *s*	6.86	0.501	0.033	0.033	2.829
Lower Bound	208.4	12.70	0.100	0.150	12.43
Upper Bound	249.5	15.70	0.300	0.350	29.40

*Bimodal distribution was observed. Equivalent values: x = 20.913 GPa, s = 2.829

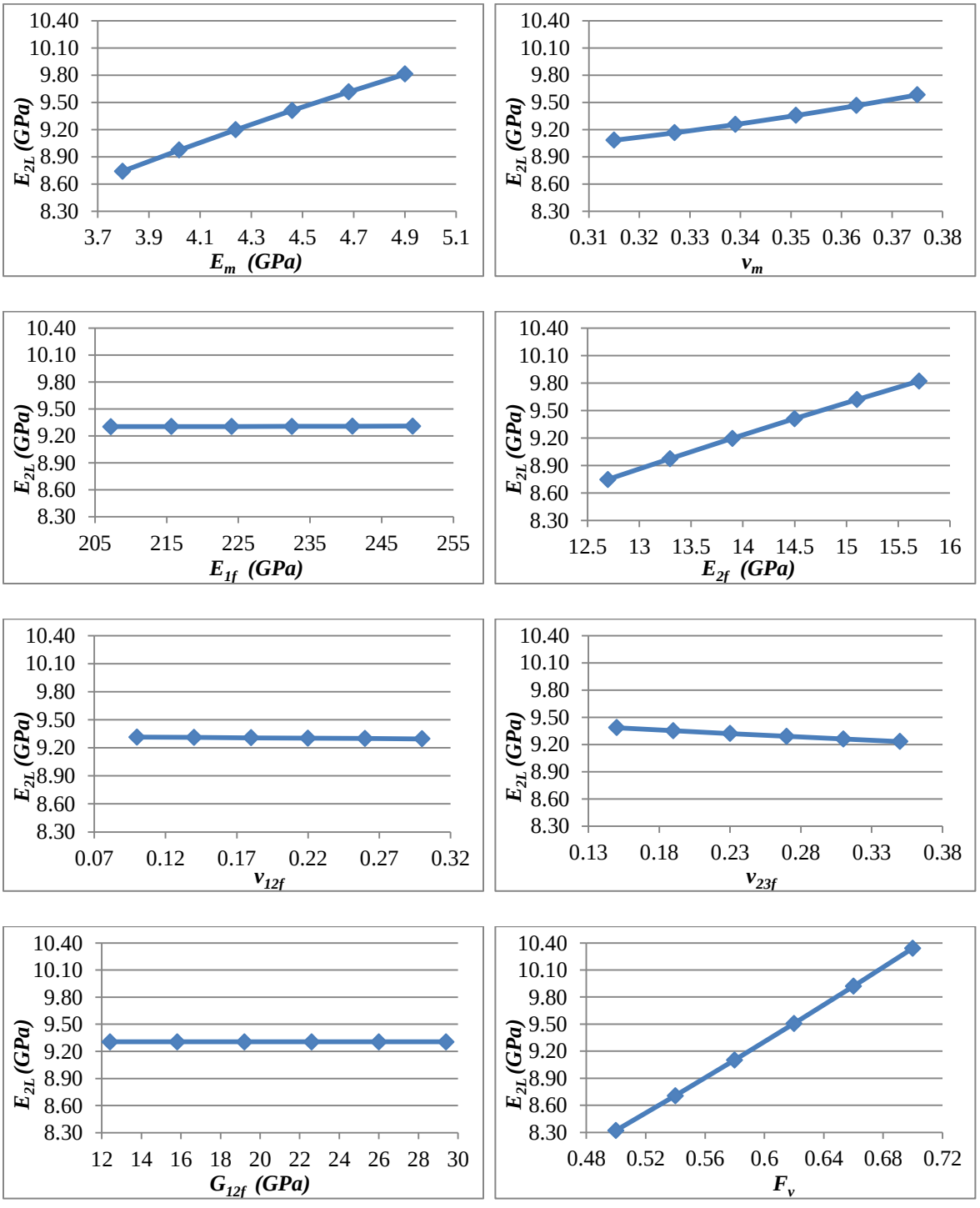

Figure 16. Sensitivity of E_{2L}

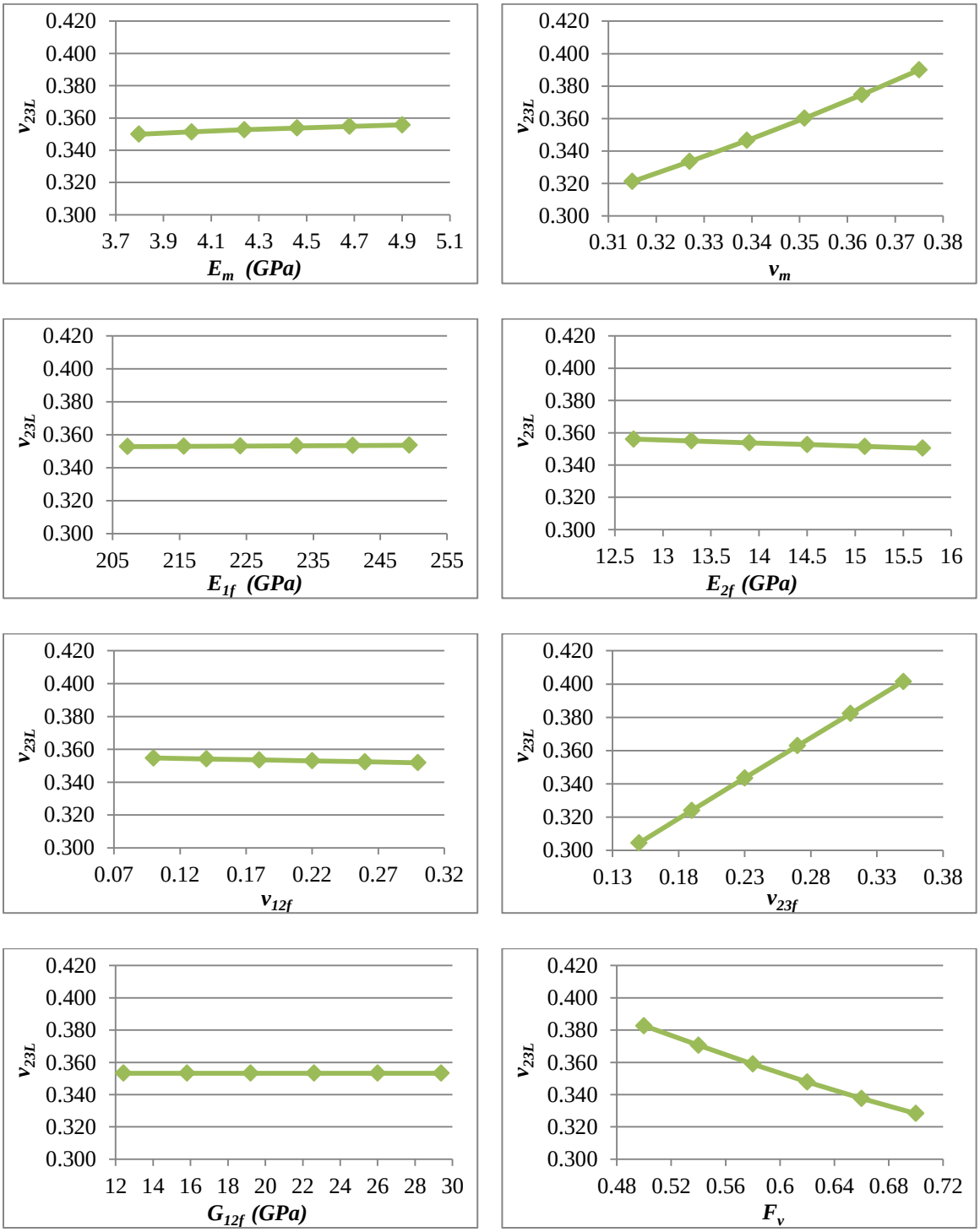

Figure 17. Sensitivity of v_{23L}

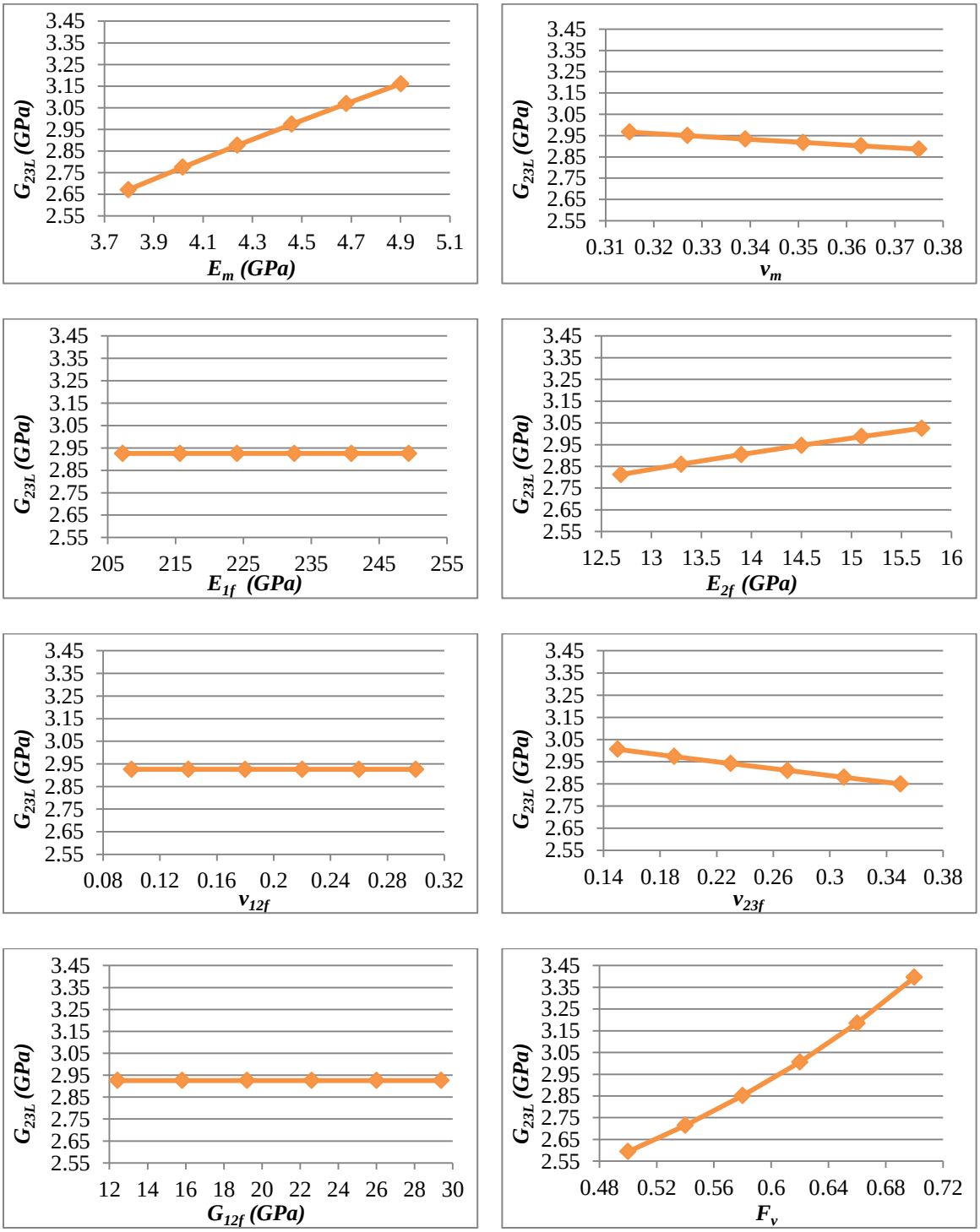

Figure 18. Sensitivity of G_{23L}

The linear relation of the sensitivities allows for the sensitivity data to be condensed into three effective sensitivity diagrams (Figures 19-21), yet a brief explanation may be necessary to fully understand each diagram. The centerline of the bar chart represents the baseline case in which the mean values for all input properties were used. Solid bars designate the decrease in the considered lamina property caused by the minimum value of the input parameter, while hatched bars designate the increase in the lamina property caused by the maximum value of the input parameter. The associated data labels were calculated as the percent change of the lamina property relative to the baseline value. For example, the data labels characterizing the influence of matrix modulus (E_m) on the transverse tensile modulus of the lamina (E_{2L}) were calculated as such.

$$\%\bar{\Delta}E_{2L} = \frac{\left|E_{2L}(min) - E_{2L}(base)\right|}{E_{2L}(base)} \cdot 100 \qquad \%\vec{\Delta}E_{2L} = \frac{\left|E_{2L}(max) - E_{2L}(base)\right|}{E_{2L}(base)} \cdot 100$$

The fiber volume ratio is clearly observed to have the strongest impact on the out-of-plane lamina properties. An influence rank is assigned to each remaining parameter by averaging its influence on all three out-of-plane lamina properties. The out-of-plane Poisson's ratio of the fiber (v_{23f}) ranks second followed by the matrix modulus (E_m), matrix Poisson's ratio (v_m), and the out-of-plane fiber modulus (E_{2f}).

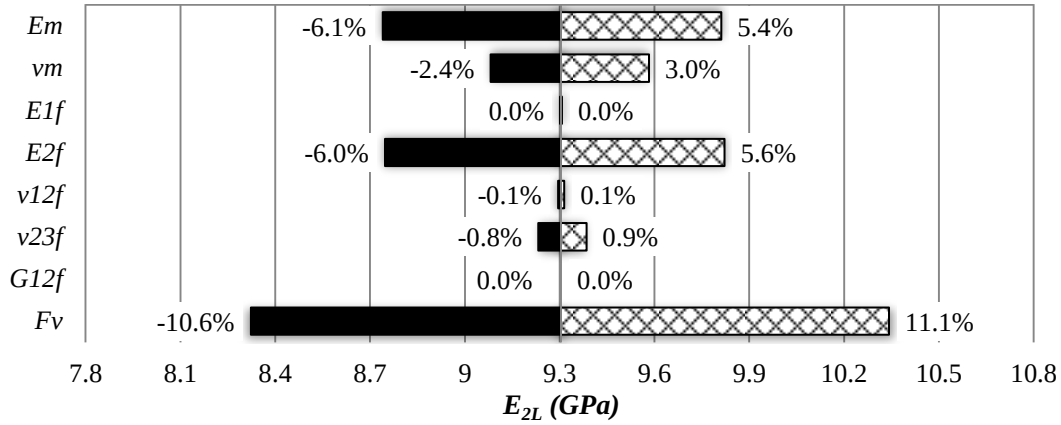

Figure 19. Sensitivity of E_{2L} Relative to Constituent Properties

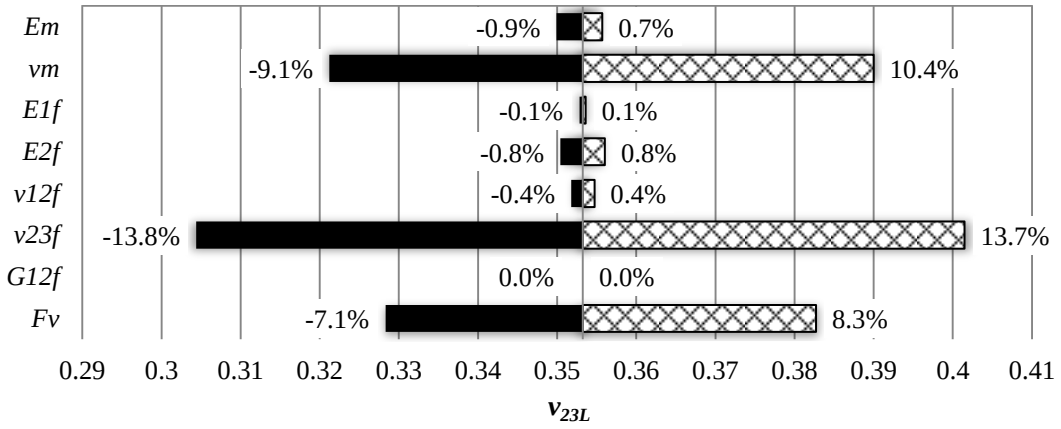

Figure 20. Sensitivity of v_{23L} Relative to Constituent Properties

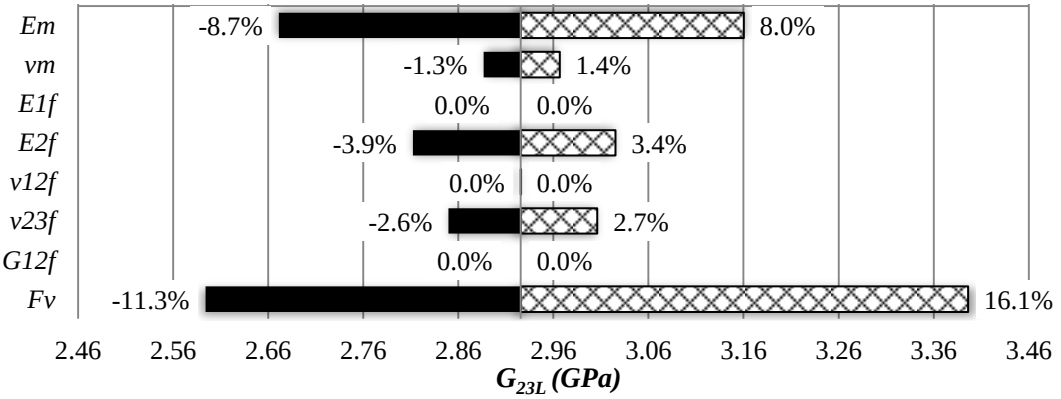

Figure 21. Sensitivity of G_{23L} Relative to Constituent Properties

The established range for each input caused considerable influence on the out-of-plane lamina properties; however, with this high fidelity analysis, it cannot be determined if the variation in the out-of-plane lamina properties is significant enough to effect overall part performance. This unit cell modeling framework acts to bridge between constituent level and lamina level properties, yet the framework must further be coupled with larger scale analyses to evaluate the influence on structural performance.

It is important to note that a total of 96 simulations are performed to gather the effective out-of-plane lamina properties, yet the total simulation time amounts to less than 29 minutes (~18 seconds per simulation). The simulations require limited computing resources, and an average laptop computer is able to perform other tasks during simulation with no noticeable slow down.

Conclusion

An automated FE based approach is developed and used to evaluate the sensitivity of out-of-plane composite lamina properties relative to constituent material properties. The modeling approach is shown to strongly agree with prior analysis results and proves to be a feasible and effective means of studying composite lamina properties. The developed unit cell modeling tools are the first in a line of multi-scale modeling tools intended to study the effect material uncertainties across multiple scales.

Chapter 4

Sensitivity Analysis of Composite Lamina with Multiple Fiber Materials

Introduction

Highly customized fiber-reinforced composites exhibit promise as an adaptable, high-performing material that can be used across many industries. For example, an advanced FRC material may contain different types of reinforcing fibers such that the properties supplied by each fiber may be used to achieve an advanced engineering function [59]. To create optimized parts designed from these highly customized materials, engineers need the capability to rapidly analyze many constituent combinations and material configurations. Leveraging today's available computing resources by performing composite analysis through simulation provides a cost-effective approach to achieving this goal. An encompassing simulation environment containing all relevant constituent information such as cost, weight, mechanical properties, and pre-made FE models will allow engineers to economically explore material combinations, develop effective testing programs, and ultimately design optimized parts that satisfy multiple engineering functions.

This chapter outlines the development and application of computational modeling tools intended to help build this encompassing simulation environment. The modeling tools developed for this lamina study are similar to those discussed in the previous chapter of this thesis. The same foundation is used to develop the load schemes, boundary displacement constraints, and homogenization routine in order to obtain the

homogenized lamina properties. However, the model to be generated by the input files consists of lamina RVE comprised of multiple unit cells aligned for a square packing sequence (Figure 22). This allows the user to specify different material properties for each cell within the RVE. Code written in C++ and batch scripting are once again used to generate input files and automate the FEA process. The modeling tools are used to evaluate the out-of-plane mechanical properties of laminas consisting of variable percentages of two different fiber materials. The framework is then used to identify a combination of the two fiber types that achieves optimal out-of-plane stiffness, deflection, and weight.

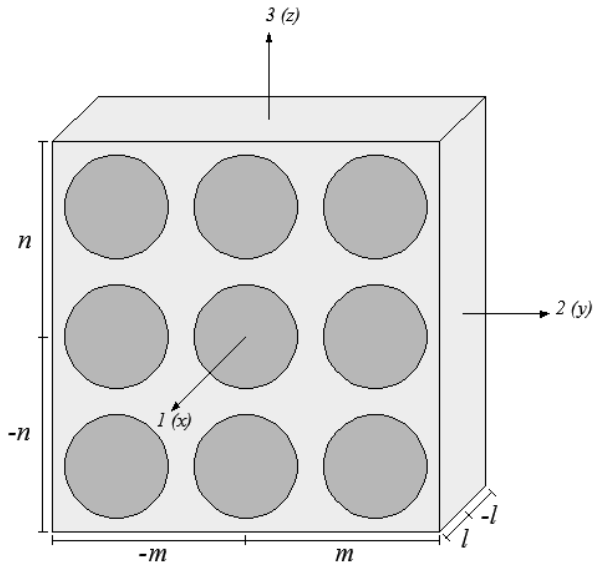

Figure 22. Example RVE of a Lamina

Finite Element Model

Model Structure

The modeling tools generate input files containing the load conditions (longitudinal and transverse tension or shear) and periodic boundary conditions in order to obtain effective lamina properties through FEA in ABAQUS. However, additional features allow the user to specify the lamina size (n rows by m columns) and material properties for each fiber in the lamina, allowing for multiple fiber types to be modeled within a single lamina RVE. As discussed in the previous chapter, the input file generation code allows the user to control mesh density, fiber volume fraction, and the applied boundary conditions (inclusion or omission of Poisson's effect). After simulations are executed, the previously outlined extraction code retrieves the boundary displacements from each model output file, calculates the homogenized properties, and deposits the results into a single CSV file.

Validation

The lamina model used for validation consists of a three by three periodic arrangement of square packed fibers. The lamina is constructed with AS4 carbon fiber and 3501-6 Epoxy each with the average properties obtained from the literature search (Table 6-7). The out-of-plane homogenized properties acquired from the lamina model are compared to the homogenized properties obtained from the unit cell model consisting of identical constituent properties. Figure 23 compares the von Mises effective stress between the two models.

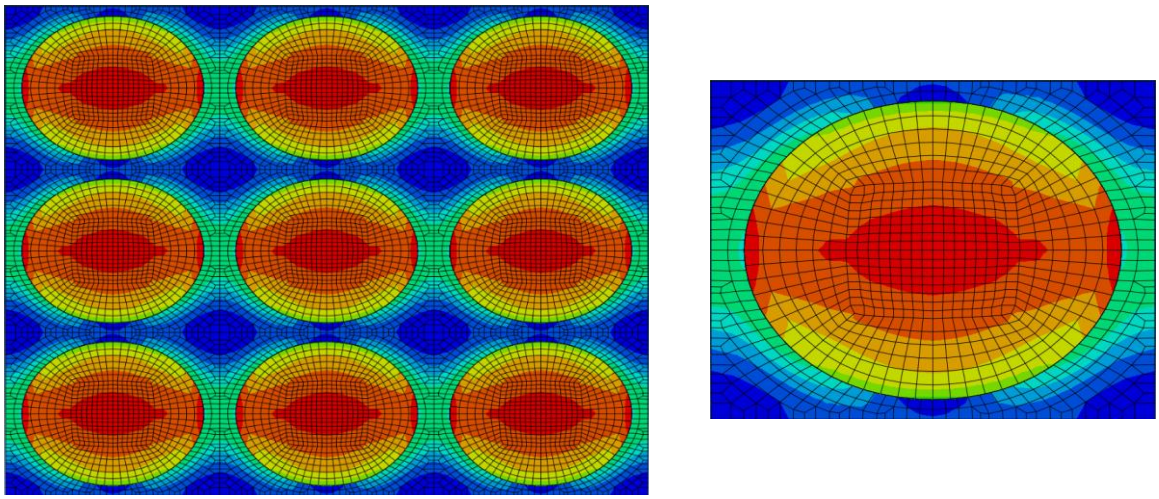

(a) Lamina in transverse tension (b) Unit cell in transverse tension

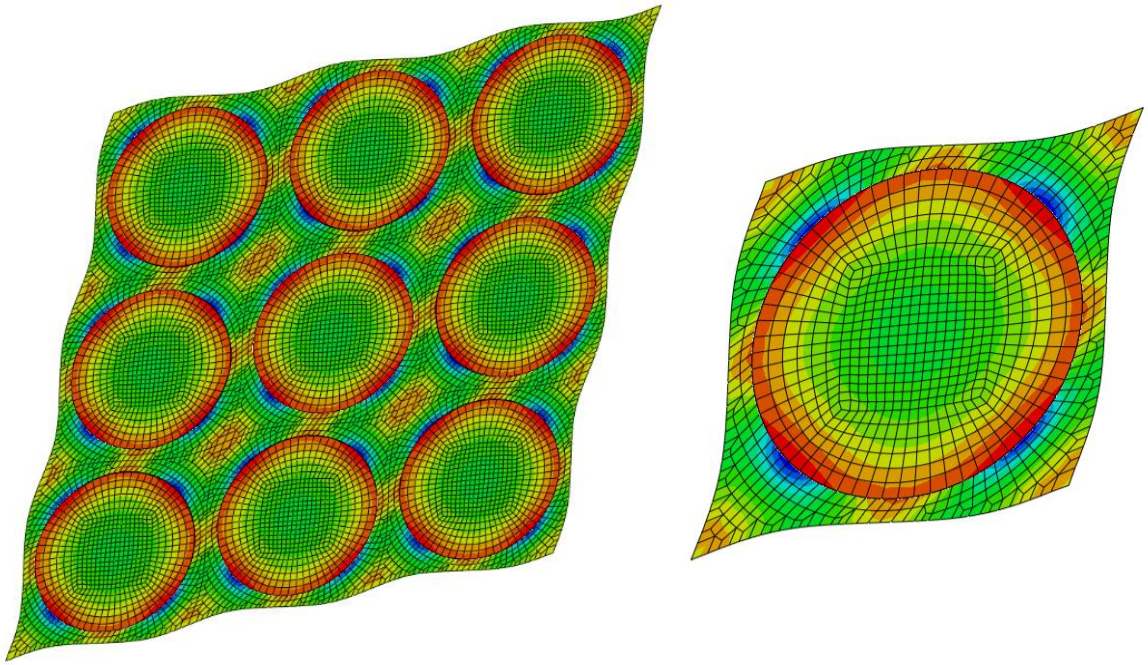

(c) Lamina in transverse shear (d) Unit cell in transverse shear

Figure 23. Comparison of Deformed Shape and Effective von Mises Stress Contours Obtained from the Lamina and Unit Cell Models

The effective stress contours, maximum and minimum effective von Mises stress, and homogenized properties are shown to agree between the models (Table 8).

Table 8. Comparison of Effective Stress and Properties Obtained from the Lamina and Unit Cell Models (AS4 Carbon / 3501-6 Epoxy)

Model	Max. Stress (Tension/Shear)	Min. Stress (Tension/Shear)	E_{2L} (GPa)	ν_{23L}	G_{23L} (GPa)
Unit Cell	1,496 / 2,165	369 / 1,007	9.305	0.353	2.928
Lamina	1,496 / 2,166	369 / 1,006	9.305	0.353	2.927

Sensitivity Analysis of Composite Lamina Consisting of Multiple Fiber Types

Designing composite lamina from multiple fiber types enables an engineer to take advantage of the favorable properties possessed by each fiber material. Therefore, the modeling framework is expanded to investigate the behavior of composite lamina consisting of two different fiber materials. The two fiber materials chosen for the analysis were AS4 carbon and Kevlar-49 Aramid fiber. AS4 carbon fiber has exceptional strength and stiffness in both compression and tension, but exhibits little toughness relative to other fiber materials. Kevlar-49 fiber is known for impact resistance because of its high tensile strength and toughness and is lighter (~20%) and cheaper than AS4 carbon. However, Kevlar-49 has a relatively low compressive strength, which limits its structural applications. Therefore, combining the two fiber materials in single composite lamina could provide for a cost-effective, tough material that retains a high degree of multi-directional strength and stiffness. The average properties of the two fiber materials

are displayed in Table 9. It is important to note that AS4 carbon is substantially more resilient to deformation than Kevlar-49 for in and out-of-plane loading.

Table 9. Avg. Properties of AS4 Carbon and Kevlar-49 from Literature Search (GPa)

Fiber Material	E_{1f}	E_{2f}	ν_{12f}	ν_{23f}	G_{12f}	G_{23f}
AS4 Carbon	229.0	14.20	0.200	0.250	20.91	5.680
Kevlar-49	127.1	3.993	0.523	0.275	14.34	1.251

Fiber Percentage Study

Using the validated modeling framework, a sensitivity analyses is performed to examine the behavior of a three by three lamina consisting of an increasing percentage of Kevlar-49 fibers. Nine different composite lamina models are used to establish a spectrum of fiber combinations beginning with a lamina comprised of all AS4 carbon fibers and ending with a lamina comprised of all Kevlar-49 fibers (Figure 24). The modeling framework is then used to generate the input files for each lamina model, run the simulation in ABAQUS, and output the out-of-plane lamina properties into a single CSV file. This demonstration study focuses only on the out-of-plane properties, although the modeling framework is not limited to out-of-plane behavior. The lamina property calculations adhere to the formulation presented by Sun and Vaidya [33] and are calculated as follows (eq. 20).

$$E_{2L} = \frac{\sigma_{22}}{\varepsilon_{22}} = \frac{P_2 \cdot L}{2u_2} \qquad \nu_{23L} = -\frac{u_3}{u_2} \qquad G_{23L} = \frac{\sigma_{23}}{\gamma_{23L}} = \frac{T_{23} \cdot L}{u_2 + u_3} \tag{20}$$

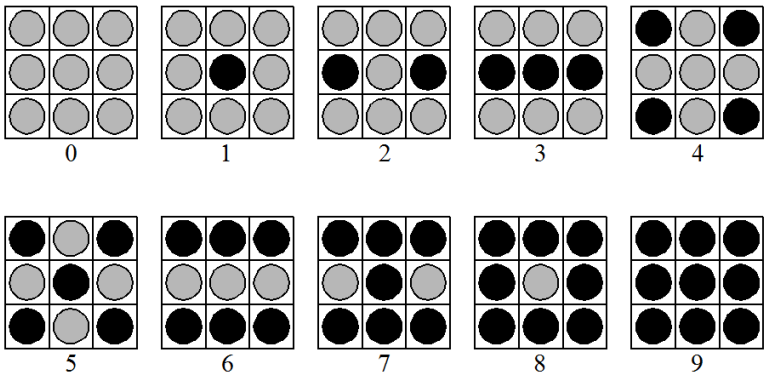

Figure 24. Lamina Combinations for Sensitivity Analysis (Black: Kevlar-49)

The terms P_2 and T_{23} are the traction loads applied to the lamina model, u_2 and u_3 are the boundary displacements obtained from the FEA, and L is the length of the lamina side. The results from the sensitivity study are displayed in Figures 25 and 26.

It is observed that the location of the stiffer fibers have a fairly substantial influence on the out-of-plane Poisson's ratio of the lamina (v_{23L}) indicated by the jump in the graph located between configuration 4 and 5. The jump in v_{23L} is due to the centrally located AS4 carbon fiber that is present in lamina combination 4, but not present in lamina combination 5. Although this is not intuitive or obvious, the AS4 carbon fibers acting in series limit the relative vertical contraction (u_3) in the lamina more profoundly than the horizontal extension (u_2).

The automation and extraction tools allow the user to identify optimal material combinations. The usefulness is demonstrated through a simple design optimization problem, where the goal is to identify a material combination that weighs less and possesses higher toughness than a traditional carbon-epoxy composite, but retains a high degree of stiffness. Just by examining the previously generated sensitivity results it is

observed that the AS4 carbon/Kevlar-49 combination just above 40% Kevlar-49 provides the maximum transverse modulus (E_{2L}) and minimal transverse Poisson's ratio (ν_{23L}). Figure 27 displays a normalized plot of the transverse modulus compared to the total composite weight, and from this figure it is observed that the combination to maximize E_{2L} and minimize weight also occurs just above 40% Kevlar-49. Therefore, it is determined that a combination consisting of 4 Kevlar-49 fibers to every 5 AS4 carbon fibers accomplishes the design goals. From a pure volumetric consideration, this combination should culminate in a 20% increase in composite lamina toughness.

While manufacturing a composite material with an exact fiber configuration is unrealistic, manufacturing materials with reasonable degree of accuracy in fiber composition is feasible.

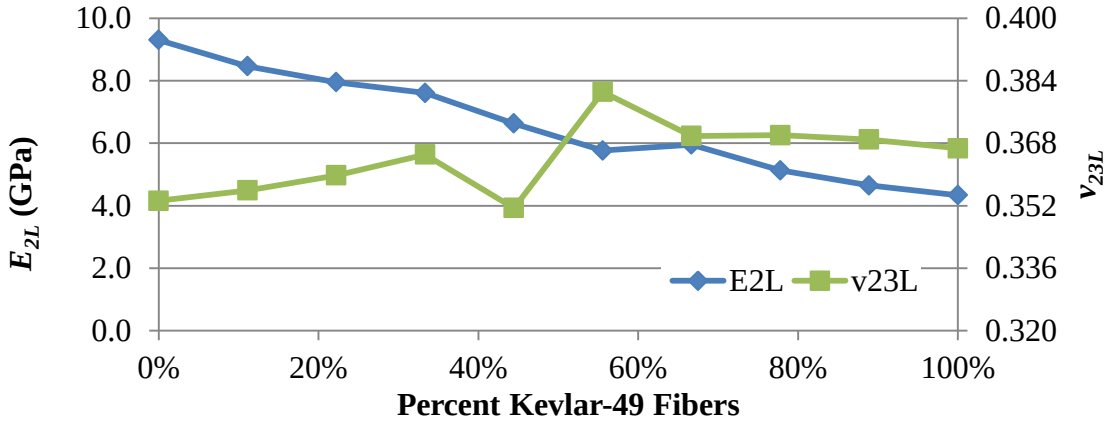

Figure 25. Effect of Increasing Kevlar-49 Percentage on E_{2L} and v_{23L}

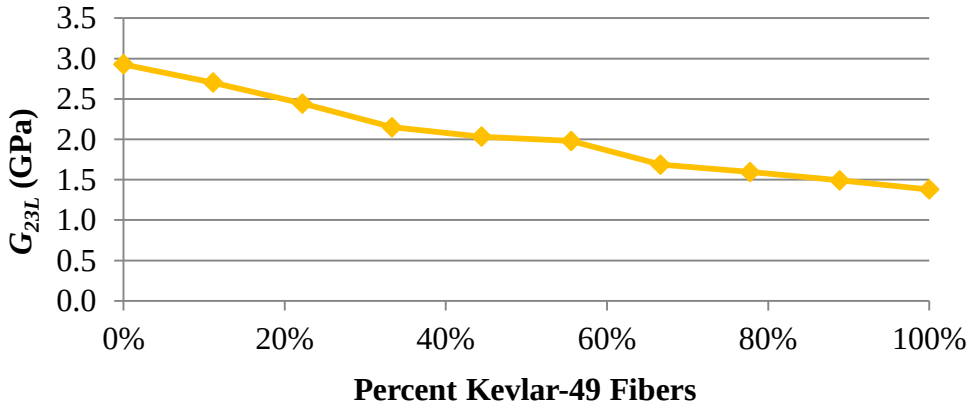

Figure 26. Effect of Increasing Kevlar-49 Percentage on G_{23L}

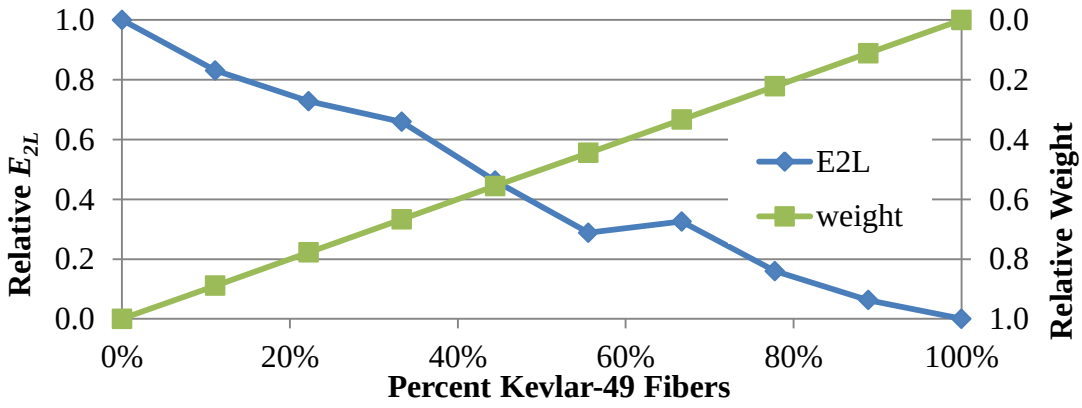

Figure 27. Bi-Fiber Lamina Optimization Problem

Fiber Configuration Study

In this section, configuration refers to the location of the different fiber materials within the lamina RVE. An analysis was performed to examine the effect of fiber configuration on the out-of-plane lamina properties because the location of the stiffer fibers appeared to cause considerable influence on the out-of-plane lamina properties (E_{2L} and v_{23L}). Several lamina models were configured consisting of exactly four AS4 carbon and five Kevlar-49 fibers randomly located throughout a lamina RVE (Figure 28).

The influence of configuration on the out-of-plane lamina properties is displayed in Figure 29. It was observed that configuration alone played a minimal role in the effective out-of-plane lamina properties. The percentage difference between the maximum and minimum achieved E_{2L} was calculated to be just 4.2%, while the percentage difference between the maximum and minimum v_{23L} was calculated to be 13.8%.

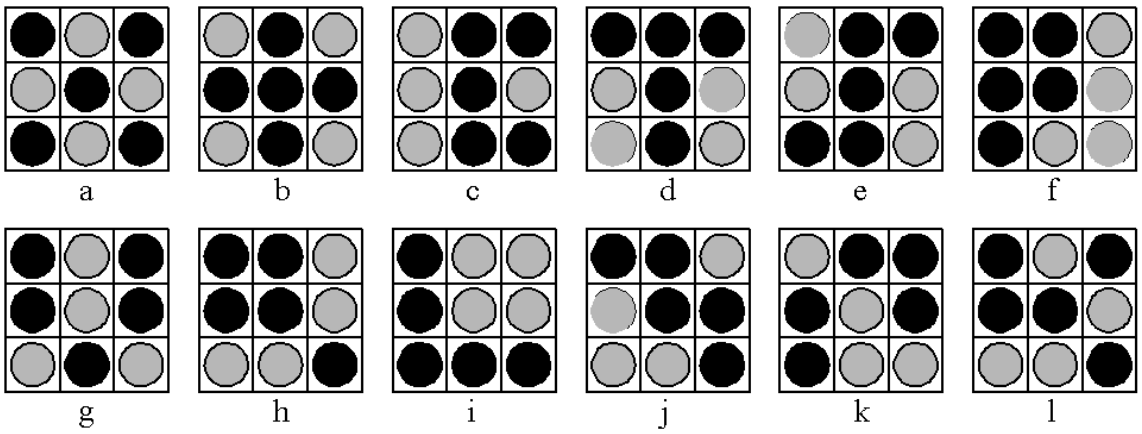

Figure 28. Lamina Configurations for Sensitivity Analysis (Black: Kevlar-49)

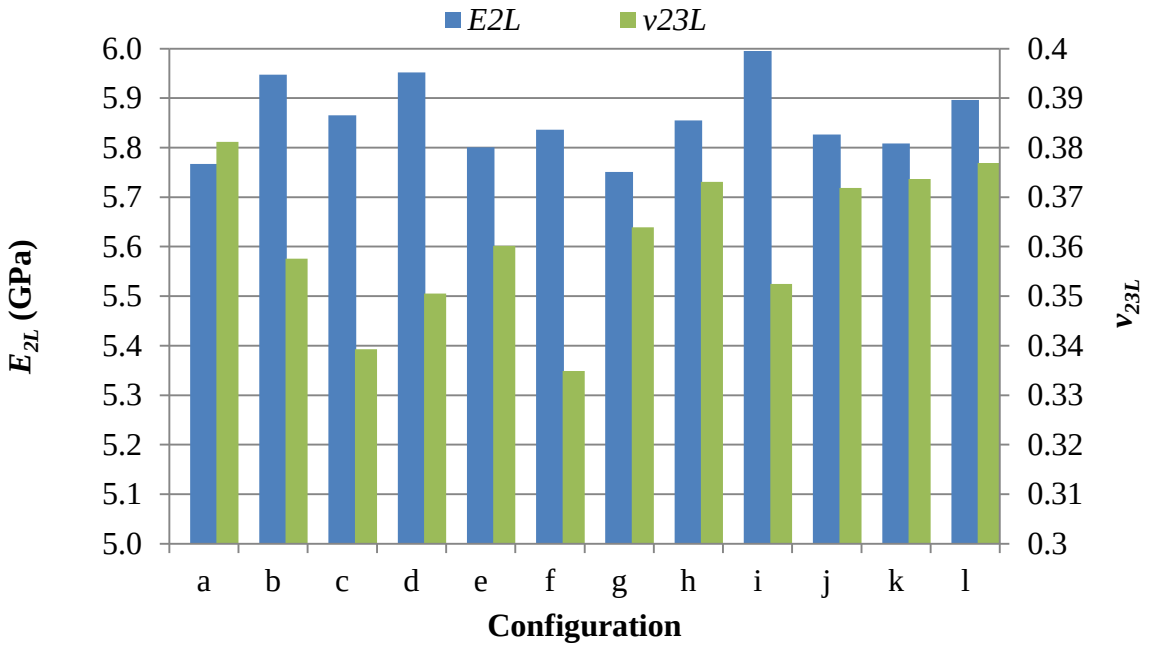

Figure 29. Effect of Configuration on E_{2L} and v_{23L}

Conclusion

The developed FE modeling framework is extended to study composite lamina. The modeling tools applied at the lamina level are shown to agree with results obtained at the unit cell level. A lamina sensitivity analysis is performed to quantify the influence of combining two different fiber materials on the out-of-plane properties and identify an optimal combination to minimize weight and stiffness and introduce toughness. The sensitivity analysis reveals that the location of the stiffer fibers may have a considerable influence on the out-of-plane lamina properties; however, an additional study challenged this notion. While the framework is capable of effectively characterizing lamina properties, the meshing algorithm only generates lamina RVEs with square fiber distribution and constant fiber diameter.

Chapter 5

Conclusion

Fiber reinforced composites are an engineered material in which a multitude of fiber and matrix materials can be chosen to create a highly customized part that meets extreme design criteria. Some of the advantages of fibrous composites consist of high specific strength and stiffness, low thermal and electrical conductivity, corrosion resistance, and enhanced fatigue life. However, fibrous composite materials are more challenging to design, command extensive testing programs to understand behavior, and require more time and resources to manufacture than traditional structural materials such as concrete, steel, and aluminum. Establishing modeling tools and design guidelines to help engineers design composite materials is an essential step toward being able to utilize fibrous composites and their many advantageous properties to meet the high engineering demands of the future. Numerical simulation methods have already been shown to provide accurate composite property prediction, and with the continual advancement of computing resources and efficiency, the application of numerical simulation methods to model complex material behaviors are seemingly endless.

List of References

1. Hashin, Z. and B.W. Rosen, *The Elastic Moduli of Fiber-Reinforced Materials.* Journal of Applied Mechanics, 1964. **31**(2): p. 223-232.
2. Singh, B., M. Gupta, and A. Verma, *Mechanical behaviour of particulate hybrid composite laminates as potential building materials.* Construction and Building Materials, 1995. **9**(1): p. 39-44.
3. Daniel, I.M. and O. Ishai, *Engineering Mechanics of Composite Materials*. 2 ed. 2006, New York: Oxford University Press.
4. Tarnopol'skii, Y.M. and V.L. Kulakov, *Tests Methods for Composites. Survey of Investigations Carried out in the PMI of Latvian Academy of Sciences in 1964-2000.* Mechanics of Composite Materials, 2001. **37**(5-6): p. 431-448.
5. Erni, J., *The Development of Unidirectional and Multidirectional Compite Modelings Using a Modified Weibull Failure Distribution; Theory, Analysis and Applications*, 2007, Arizona State University.
6. Averill, R.C. and G.P. Carman, *Analytical Modeling of Micromechanical Stress Variations in Continuos Fiber-Reinforced Composites*, in *Local Mechanics Concepts for Composite Material Systems*, J.N. Reddy and K.L. Reifsnider, Editors. 1992, Springer Berlin Heidelberg. p. 27-61.
7. Hashin, Z., *The Elastic Moduli of Heterogenous Materials*, 1960, Harvard University.
8. Zhang, W.-C. and K.E. Evans, *An analytical model for the elastic properties of fibrous composites with anisotropic constituents.* Composites Science and Technology, 1990. **38**(3): p. 229-246.
9. Dong, X.N., et al., *A generalized self-consistent estimate for the effective elastic moduli of fiber-reinforced composite materials with multiple transversely isotropic inclusions.* International Journal of Mechanical Sciences, 2005. **47**(6): p. 922-940.
10. Chamis, C.C., *Simplified composite micromechanics equations of hygral, thermal, and mechanical properties.* Sampe Quarterly, 1984. **15**: p. 14-23.
11. Markov, K., *Elementary Micromechanics of Heterogeneous Media*, in *Heterogeneous Media*, K. Markov and L. Preziosi, Editors. 2000, Birkhäuser Boston. p. 1-162.
12. Tyrus, J.M., M. Gosz, and E. DeSantiago, *A local finite element implementation for imposing periodic boundary conditions on composite micromechanical models.* International Journal of Solids and Structures, 2007. **44**(9): p. 2972-2989.
13. Jeanmeure, L. and S. Li, *AUTOMATED GENERATION OF EQUATION-BASED BOUNDARY CONDITIONS FOR MULTISCALE MODELLING OF UNIT CELLS.*
14. Nguyen, V.D., et al., *Imposing periodic boundary condition on arbitrary meshes by polynomial interpolation.* Computational Materials Science, 2012. **55**(0): p. 390-406.
15. Li, S., *Boundary conditions for unit cells from periodic microstructures and their implications.* Composites Science and Technology, 2008. **68**(9): p. 1962-1974.
16. Kurukuri, S., *A comprehensive study: Boundary conditions for representative volume elements (RVE) of composites*, Institute of Structural Mechanics. p. 13.

17. Kirkup, S. and J. Yazdani. *A gentle introduction to the boundary element method in MATLAB/FREEMAT*.
18. Kamiński, M., *Sensitivity and randomness in homogenization of periodic fiber-reinforced composites via the response function method.* International Journal of Solids and Structures, 2009. **46**(3–4): p. 923-937.
19. Kamiński, M., *Boundary element method homogenization of the periodic linear elastic fiber composites.* Engineering Analysis with Boundary Elements, 1999. **23**(10): p. 815-823.
20. Okada, H., Y. Fukui, and N. Kumazawa, *Homogenization method for heterogeneous material based on boundary element method.* Computers & Structures, 2001. **79**(20–21): p. 1987-2007.
21. Chen, X. and Y. Liu, *Multiple-cell modeling of fiber-reinforced composites with the presence of interphases using the boundary element method.* Computational Materials Science, 2001. **21**(1): p. 86-94.
22. Cook, R.D., *Finite Element Modeling for Stress Analysis*. 1995, New York: Wiley.
23. King, T.R., et al., *Micromechanics Prediction of the Shear Strength of Carbon Fiber/Epoxy Matrix Composites: The Influence of the Matrix and Interface Strengths.* Journal of Composite Materials, 1992. **26**(4): p. 558-573.
24. Blackketter, D.M., D. Upadhyaya, and T.R. King, *Micromechanics prediction of the transverse tensilc strength of carobn fiber/epoxy composites: The influence of the matrix and interface.* Polymer Composites, 1993. **14**(5): p. 437-446.
25. Karami, G. and M. Garnich, *Effective moduli and failure considerations for composites with periodic fiber waviness.* Composite Structures, 2005. **67**(4): p. 461-475.
26. Garnich, M.R. and G. Karami, *Finite Element Micromechanics for Stiffness and Strength of Wavy Fiber Composites.* Journal of Composite Materials, 2004. **38**(4): p. 273-292.
27. Medeiros, R.d., et al., *Effective properties evaluation for smart composite materials.* Journal of the Brazilian Society of Mechanical Sciences and Engineering, 2012. **34**: p. 362-370.
28. Naik, A., et al., *Micromechanical Viscoelastic Characterization of Fibrous Composites.* Journal of Composite Materials, 2008. **42**(12): p. 1179-1204.
29. Caruso, J.J., *Application of finite element substructuring to composite micromechanics*. 1984, [Washington, D.C.?: National Aeronautics and Space Administration.
30. Brockenbrough, J.R.S.S.W.H.A., *Deformation of metal-matrix composites with continuous fibers : geometrical effects of fiber distribution and shape*. 1990, s.L.: Alcoa.
31. Naik, R.A. and J.H. Crews Jr., *Micromechanical analysis of fiber-matrix interface stresses under thermo-mechanical loadings*, in *Composite Materials: Testing and Design*, E.T.C. Jr., Editor 1993, American Society for Testing and Materials: Philadelphia, PA. p. 14.

32. Adams, D.F. and D.A. Crane, *Finite element micromechanical analysis of a unidirectional composite including longitudinal shear loading.* Computers & Structures, 1984. **18**(6): p. 1153-1165.
33. Sun, C.T. and R.S. Vaidya, *Prediction of composite properties from a representative volume element.* Composites Science and Technology, 1996. **56**(2): p. 171-179.
34. Drago, A. and M.-J. Pindera, *Micro-macromechanical analysis of heterogeneous materials: Macroscopically homogeneous vs periodic microstructures.* Composites Science and Technology, 2007. **67**(6): p. 1243-1263.
35. Taliercio, A., *Generalized plane strain finite element model for the analysis of elastoplastic composites.* International Journal of Solids and Structures, 2005. **42**(8): p. 2361-2379.
36. Theocaris, P.S., G.E. Stavroulakis, and P.D. Panagiotopoulos, *Calculation of effective transverse elastic moduli of fiber-reinforced composites by numerical homogenization.* Composites Science and Technology, 1997. **57**(5): p. 573-586.
37. Xu, Y., et al., *Evaluation of the effective elastic properties of long fiber reinforced composites with interphases.* Computational Materials Science, 2012. **61**(0): p. 34-41.
38. Würkner, M., H. Berger, and U. Gabbert, *Numerical study of effective elastic properties of fiber reinforced composites with rhombic cell arrangements and imperfect interface.* International Journal of Engineering Science, 2013. **63**(0): p. 1-9.
39. Xia, Z., Y. Zhang, and F. Ellyin, *A unified periodical boundary conditions for representative volume elements of composites and applications.* International Journal of Solids and Structures, 2003. **40**(8): p. 1907-1921.
40. Pindera, M.-J., et al., *Micromechanics of spatially uniform heterogeneous media: A critical review and emerging approaches.* Composites Part B: Engineering, 2009. **40**(5): p. 349-378.
41. Portela, A., M.H. Aliabadi, and D.P. Rooke, *The dual boundary element method: Effective implementation for crack problems.* International Journal for Numerical Methods in Engineering, 1992. **33**(6): p. 1269-1287.
42. Sun, C.T. and J.L. Chen, *A micromechanical model for plastic behavior of fibrous composites.* Composites Science and Technology, 1991. **40**(2): p. 115-129.
43. Riley, M.B. and J.M. Whitney, *Elastic properties of fiber reinforced composite materials.* AIAA Journal, 1966. **4**(9): p. 1537-1542.
44. Sun, C.T. and S.G. Zhou, *Failure of Quasi-Isotropic Composite Laminates with Free Edges.* Journal of Reinforced Plastics and Composites, 1988. **7**(6): p. 515-557.
45. Lee, J.-W. and I.M. Daniel, *Progressive Transverse Cracking of Crossply Composite Laminates.* Journal of Composite Materials, 1990. **24**(11): p. 1225-1243.
46. Hamby, D., *A review of techniques for parameter sensitivity analysis of environmental models.* Environmental Monitoring and Assessment, 1994. **32**(2): p. 135-154.

47. Soden, P., M. Hinton, and A. Kaddour, *Lamina properties, lay-up configurations and loading conditions for a range of fibre-reinforced composite laminates.* Composites Science and Technology, 1998. **58**(7): p. 1011-1022.
48. Yim, J.H. and J. Gillespie Jr, *Damping characteristics of 0 and 90 AS4/3501-6 unidirectional laminates including the transverse shear effect.* Composite structures, 2000. **50**(3): p. 217-225.
49. Adams, D.F. and L.G. Adams, *Tensile impact tests of AS4/3501-6 and S2/3501-6 unidirectional composites and the 3501-6 epoxy matrix.* Journal of composite materials, 1990. **24**(3): p. 256-268.
50. Guagliano, M. and E. Riva, *Mechanical behaviour prediction in plain weave composites.* The Journal of Strain Analysis for Engineering Design, 2001. **36**(2): p. 153-162.
51. Nicoletto, G. and E. Riva, *Failure mechanisms in twill-weave laminates: FEM predictions vs. experiments.* Composites Part A: Applied Science and Manufacturing, 2004. **35**(7–8): p. 787-795.
52. *3501-6 Epoxy Matrix Product Data*, Hexcel, Editor 1998.
53. Gipple, K. and D. Hoyns, *Measurement of the out-of-plane shear response of thick section composite materials using the V-notched beam specimen.* Journal of composite materials, 1994. **28**(6): p. 543-572.
54. Bauccio, M., *ASM engineered materials reference book*. 1994: ASM International.
55. Wessel, J.K., *The handbook of advanced materials: enabling new designs*. 2004: John Wiley & Sons.
56. Reinhart, T.J. and A.I.H. Committee, *Engineered Materials Handbook: Composites*. 1987: ASM International.
57. *HexTow AS4D Carbon Fiber Product Data*, Hexcel, Editor 2010.
58. Mallick, P.K., *Composites Engineering Handbook*. 1997: Taylor & Francis.
59. Hayes, B.S. and L.M. Gammnon, *Optical Microscopy of Fiber-Reinforced Composites*. 2010: ASM International.

Vita

Jonathan Weigand was born in Maryville, TN. He attended the University of Tennessee in Knoxville where he obtained a Bachelor of Science degree in Civil Engineering graduating as a Top Collegiate Scholar for his academic performance. Jonathan went on to study computational structural mechanics within the Civil Engineering department at the University of Tennessee. He worked as a teaching assistant and graduate researcher while working to complete his Master of Science in Civil Engineering.